Turbidity Dynamics during High-Flow Storm Events in the Clackamas River, Oregon 2006-2012

Micelis Clyde Doyle
Portland State University

Recommended Citation
Doyle, Micelis Clyde, "Turbidity Dynamics during High-Flow Storm Events in the Clackamas River, Oregon 2006-2012" (2017). *Dissertations and Theses.* Paper 3884.
https://doi.org/10.15760/etd.5772

Turbidity Dynamics during High-Flow Storm

Events in the Clackamas River, Oregon 2006-2012

by

Micelis Clyde Doyle

A thesis submitted in partial fulfillment of the
requirements for the degree of

Master of Science
In
Environmental Science and Management

Thesis Committee:
Heejun Chang, Chair
J. Alan Yeakley
Yangdong Pan

Portland State University
2017

Abstract

Turbidity is a useful parameter that can be utilized to help understand the water quality in a river and is an expression of the optical properties of a liquid that cause light rays to be scattered and absorbed rather than transmitted in straight lines. A total of 41 storm events occurring during water years 2006-2012 were analyzed for this study. A hysteresis index (HI) was used to assess the difference in turbidity on the rising and falling limbs of a storm-hydrograph. The upstream Carter Bridge site exhibited a clockwise (C) hysteresis in 38 of 41 storm events and counter-clockwise (CC) hysteresis in three storm events. The downstream Oregon City site exhibited clockwise hysteresis in 29 of 41 storm events and counter-clockwise hysteresis in 12 storm events. Paired t-test comparisons of calculated HI measured during storm events showed that the upstream forested site Carter Bridge had a statistically significant higher HI than the downstream Oregon City site, suggesting that particles that contribute to increasing turbidity and suspended sediment at the upstream site are delivered to the river earlier in the storm event in comparison to the downstream Oregon City site. In contrast particulate matter and suspended sediment was more likely to be higher on the receding limb of the storm hydrograph at the downstream site in comparison to the upstream monitoring location.

Multiple linear regression analysis determined the major hydrological controls influencing turbidity over the period of a storm event. The log value of the change (Log

ΔQ) in discharge explained 81% of the log value of change in turbidity (Log ΔTb) at Carter Bridge and 48% of the change in turbidity at Oregon City for all storms. Log ΔQ explained 85% and 50% variations of Log ΔTb at Carter Bridge and at Oregon City, respectively in the wet season. Log ΔQ explained 82% of Log ΔTb at Carter Bridge during the Dry Season and together with 3-day antecedent precipitation, Log ΔQ explained 84% of variation in Log ΔTb at Oregon City during the Dry Season. The findings of this study, which offers information about the dynamics that lead to increased turbidity events, could be helpful to researchers, regulatory agencies and water resource managers in maintaining high water quality in rivers.

Dedication

I would like to dedicate this thesis to my immediate family Kate, Malik and Mia who had to deal with me typing away in my office when they wanted to spend time with me. They certainly need to understand that the feeling was mutual and I will make up for it. I would also like to dedicate this to my friends and family that continued to support me and give me encouragement throughout this long process. I could not have done this without all of you.

Acknowledgments

Table of Contents

LIST OF TABLES

LIST OF FIGURES

1. Introduction

Turbidity is a measure of the collective optical properties of a water sample that cause light to be scattered and absorbed rather than transmitted in straight lines. The higher the concentration of suspended particles, the higher the scattering and absorbance of light, and thus, the higher the turbidity value of the water sample. Primary contributors to turbidity include clay, silt, finely divided organic and inorganic matter, soluble colored organic compounds, plankton, and microscopic organisms (American Public Health Association and others, 1998). Turbidity is caused by sediment erosion, sediment resuspension and other particulate matter affecting the clarity of a water sample. Basin geology and soil composition, land-use and soil exposure, slope of a river channel, geomorphic structure of the channel, precipitation and runoff, origin of the water including point and nonpoint sources are all components that affect the turbidity observed in rivers and streams. A conceptual model of the environmental influences that affect turbidity are represented in Figure 1.
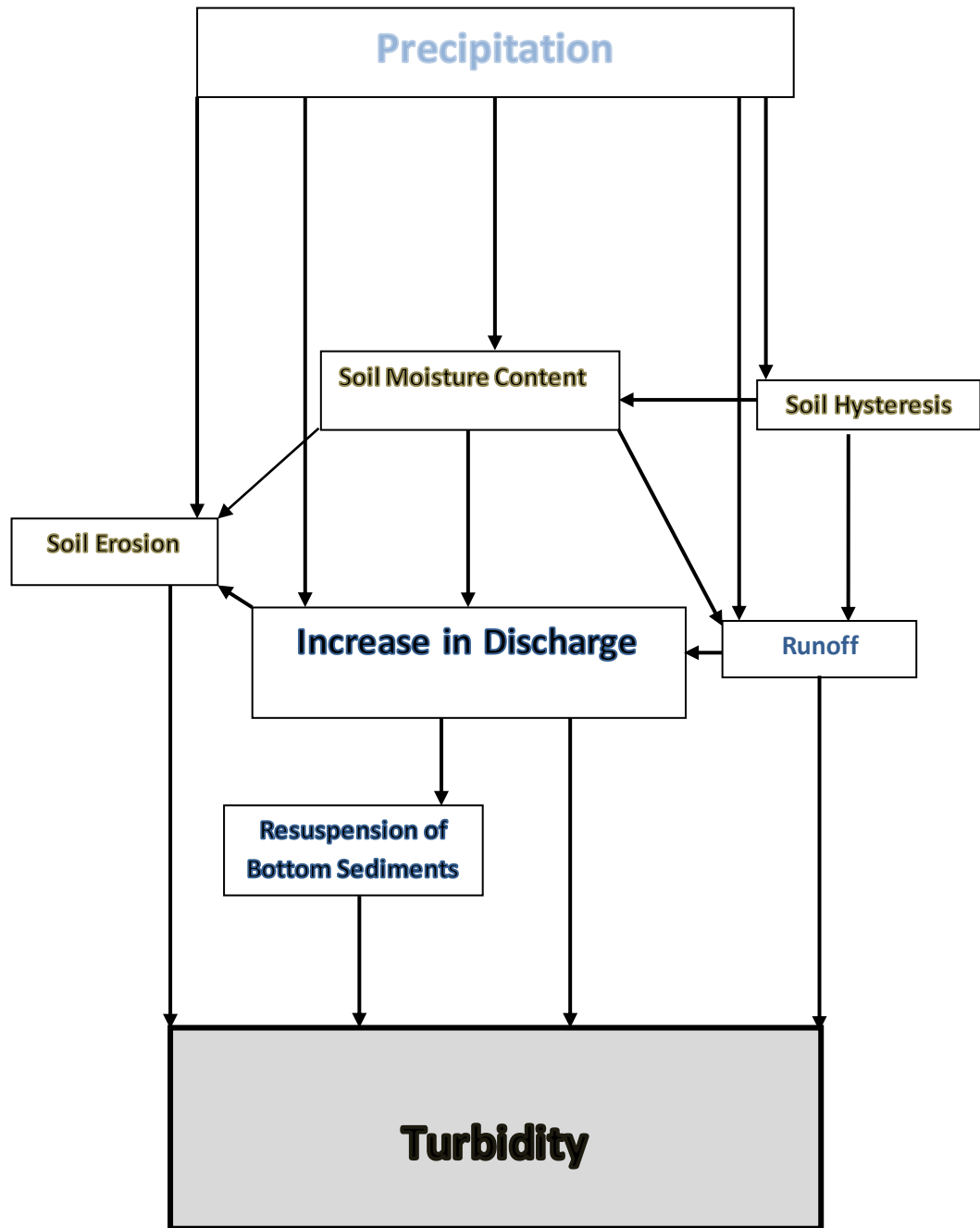
Figure 1. Conceptual model of elements that contribute to increased turbidity during storm events

Turbidity measured in river waters during storm events exhibits a close positive relationship with suspended sediment concentration (SSC). Many studies have used turbidity measurements as a surrogate to calculate suspended sediment loads in rivers and streams (Wass et al., 1997, Uhrich et al., 2003, Chanson and Takeuchi, 2008, Uhrich and Kolasinac, 2014). This process involves measuring turbidity while simultaneously collecting water samples that are then analyzed for SSC. After the collection of sufficient samples, linear regression models are often used to calculate sediment loads (Bragg, 2007). Particle size, shape and composition can all be expected to influence light attenuation and turbidity, so any attempt to use turbidity measurements as a surrogate for direct determinations of SSC should take careful account of such factors (Gippel, 1989).

Increases in turbidity readings regularly occur during storm events when rainfall and storm runoff mobilize particles from the riparian zone, upstream locations in the watershed and the overall stream network within a catchment (Chen and Chang 2014). Water from storm events and related runoff can increase river discharge and flow velocity. Increases in discharge are associated with increased shear velocities and turbulence and therefore an increased capacity to erode and transport sediment. Soil erosion and subsequent sediment transport into a waterway involves detachment, entrainment and eventual transport of particles via the stream network. The sources of sediment and particulate matter contributing to elevated turbidity readings can have an impact on the water quality of rivers, because various types of chemical compounds can

be adsorbed onto the surface of sediment particles. Sediment, solids and other particulate matter can act as a substrate for transport of pollutants such as heavy metals (Horowitz, 1991), nutrients such as total phosphorus, bacteria (*E. Coli*), (Anderson and Rounds, 2003), nutrients (McKee and others, 2000), hydrocarbons and pesticides (Larson, 1997, Settle and Ashantha, 2007). Sediment and sediment-associated constituents are leading pollutants impacting waterbodies and undermining their values and functions for habitat, water supply, recreation, energy production, navigation and other functions (Fletcher and Deletic, 2007). Estimating the mass of pollutants (e.g. nutrients, heavy metals and sediment) is a prerequisite to the effective management of water quality in waterways (Fletcher and Deletic, 2007).

A number of studies have shown that a majority of annual sediment transport can occur during high flow storm events (Richards and Holloway, 1987; Longabucco and Rafferty, 1998; Davies-Colley and Smith, 2001; O'Donnell and Effler, 2006) (see Table 1). The dominant control on suspended sediment concentration is the supply of material to the river. The existence of a relationship between concentration and discharge is a reflection of the fact that sediment supply increases during periods of precipitation and storm runoff (Berrie, 1993). These periods are generally characterized by high discharges. These periods of high discharge will reflect not only land-use, soil and the underlying rock mineralogy, but also the antecedent soil moisture conditions as well as the spatial intensity and duration of rainfall (House and Warwick, 1998).

Antecedent precipitation is precipitation falling before, but influencing the runoff yields of a given rainfall event. An antecedent precipitation index (API) is often used for the estimation of runoff yields from rainfall events on those watersheds whose auxiliary data are limited, or are not available (Ali et al., 2010). The importance of antecedent rainfall during intervals prior to the start of a rainstorm, in controlling the infiltration capacity of the soil profile and the initiation of runoff has been recognized for years (Istok and Boersma, 1986). The antecedent soil water content affects the infiltration rate. Wet soil has a lower infiltration rate than a dry soil. Precipitation falling on a wet soil will result in a higher runoff rate than the same amount of precipitation falling on a dryer soil.

Hysteresis in relation to soil moisture content is due to the fact that during soil wetting; the small pores fill first, while during drainage and drying the large pores empty first. Soil water hysteresis has a different relationship between soil water and soil suction during wetting and drying and will vary depending on the wetting and drying history of the soil (Ward and Trimble, 2004). As the pore size fills with water, the infiltration capacity of the soil profile decreases. Any additional rainfall occurring after soil saturation immediately becomes, runoff even if the rainfall intensity is very small (Istok and Boesrma, 1986). Hysteresis patterns in the relationship of discharge to suspended concentration have been investigated in efforts to understand the factors leading to the discharge-sediment transport patterns (Seeger et al., 2004).

According to Nistor and Church (2005), the most common pattern is the clockwise hysteresis that indicates depletion of available sediment before the stream flow peak occurs. Counterclockwise hysteresis indicates delayed sediment travel time resulting from the downstream distance of the measuring station from the sediment source (Williams, 1989). According to Asselman (1999), suspended sediment originating from the stream channel typically causes larger turbidity values during the rising limb of a stream flow peak (clockwise hysteresis), and sediment originating from more distant basin sources often causes larger turbidity values during the falling limb (counterclockwise hysteresis) of the storm hydrograph. The amount of particulate matter entrained in runoff is a chief determinant in turbidity to rivers during storm events.

Understanding the dynamics that lead to increased turbidity events can be helpful to researchers, regulatory agencies and water resource managers in maintaining high water quality in rivers such as the Clackamas River.

Table 1.   **Representative studies investigating turbidity dynamics, hysteresis and suspended sediment during storm events**

Authors	Study area (size)/Land Use	Data Used	Methods	Findings
J.D. ISTOK and L. BOERSMA	5-watersheds from 0.46-285 hectares . Slopes ranging from 4-15% and moderately deep, well drained deposits of silty material overlying a paleosol or weathered tuffaceous sandstone. No specific land use information provided, but based on location in an experimental watershed in Polk County, Oregon it is likely a mostly forested area.	Various rainfall parameters to characterize rainfall intensity and rainfall magnitude	Stepwise discriminant analysis to determine the values and combinations of rainfall-event characteristics that were significant in predicting the occurrence and amount of rainfall.	Antecedent precipitation falling during the 12-120 hours preceding the event was most important variable in determining runoff. Mostly clockwise hysteresis for particulate nutrients (N and P)
Y. Tramblay1, R. Bouaicha2,	655 km^2- Forested land cover upstream and cultivated plans in the lower portions of the basin. No cities or urban areas	Estimators include an antecedent discharge index, an antecedent precipitation index and continuous daily soil moisture accounting model (SMA) to develop rainfall-runoff models to manage water storage and flooding	Modeled 16 flood events occurring over a 24-year period. Rainfall, discharge and satellite remote sensing for soil moisture using.	The best results were obtained with daily soil moisture accounting (SMA) model. Remote sensing data were deemed potentially useful to estimate the soil moisture conditions in

Authors	Study area (size)/Land Use	Data Used	Methods	Findings
J. Philip O'KANE	Conceptual model of hysteresis in hydrology. Discusses rate-dependent and rate-independent systems in the unsaturated zone of the hydrological cycle	Introduces the concept of rate-independence in a hydrological context. Shows how to insert rate-independent hysteresis in conceptual hydrological models	Details and derives equations describing hysteresis in soil physics and hydrology	Resource about for hysteretic theory. Paper explained rate-independent hysteresis that contributes to the goal of predicting hydrologic response
WILLIAM A. HOUSE**M and MELANIE S. WARWICK	One large catchment and two nested sub catchments. One site 54 km downstream. Mixed land use of Agricultural, livestock (cattle and sheep) and urban areas	Attempted to quantify and model hysteresis effect using detailed chemical and river discharge data collected at 2 hour intervals. Diffuse inputs related to discharge	Comparing nutrient samples collected during baseflow and stormflow conditions. An empirical mass-balance model on water in soil to determine magnitude and direction of concentration/discharge hysteresis	Results illustrate hysteresis effects for all of the determinants and diffuse inputs with the majority of events demonstrating clockwise' hysteresis
Authors	**Study area (size)/Land Use**	**Data Used**	**Methods**	**Findings**
Lester McKee, Bradley Eyre and Shahadat Hossain	$99,000 \text{ km}^2$ – 4 sub basins of mixed land use primarily forested and agricultural with urban areas less than 10%	Compare and contrast intra and interannual variations in nutrient loads during storm events Hysteresis explained by flushing of antecedent material and exhaustion of material during single or consecutive storms	Water samples collected for nutrient analysis nitrogen (N) and phosphorus (P) on the rising and falling limb of storm hydrograph	Particulate nitrogen and phosphorus showed a clockwise hysteresis loop during all flood events. Majority of nutrients transported during storms

Evans, C., and T.D. Davies. 1998	Data collected in Adirondacks New York and the Northern Appalachian Plateau in Pennsylvania	Models of runoff generation are used to explain this hysteresis effect and to illustrate how different component concentrations produced different hysteresis forms. Only single peak events and a minimum of two samples collected on each limb of hydrograph	Model concentration-discharge hysteresis by modeling a 3-component approach. Pre-event, event water sources-and water from the soil-zone is a third component	Concentration-Discharge relationship between groundwater, solid water and surface water
Jack Lewis and Rand Eads	5-storms in a 946 acre rain dominated watershed with mostly fine-grain sediment. Fewer than 10 storm events in a 20,000 acre basin with predominantly sand sized particles	Provide information on use, benefits and cautions of continuous turbidity measurements comparing and contrasting two basins with different sediment types	Linear regression to fit suspended sediment concentration to turbidity at 10-minute intervals	Turbidity is probably more useful than water discharge as a long-term predictor of SSC
D.M. Lawler a,*, G.E. Petts a, I.D.L. Foster b, S. Harper	Upper Tames River in West Midlands UK. Urbanized basin with numerous industrial and domestic water supply systems.	Investigating an urban headwater stream during a series of spring storms by evaluating storm-event turbidity dynamics. A hysteretic index (HI) on turbidity. Turbidity during the initial, mid and peak flow of an event was used to investigate turbidity during	15 spring storms analyzed to investigate ammonia peaks, biofilm formation, bed sediment stores using HI and assessing turbidity on rising and falling limb of the storm hydrograph	Found more counter clock-wise hysteresis in urban catchments. This contrasts with clockwise hysteresis mostly observed in more rural landscapes.

9

Authors	Study area (size)/Land Use	Data Used	Methods	Findings
		storm events.		
Paul V Bolstad and Wayne T Swank2	8.7 stream kilometers covering 5-monitoring stations of varying land use between each station. Upstream mainly deciduous forests. Other 4-stations had mix of pastures, home sites, and farmland and low density suburban mix.	Land use characterizations by using 50, 100 and 300 meter buffers. Compared baseflow and stormflow concentrations of various water quality and chemical constituents to compare downstream changes in water quality during storms	Nutrient, metals, field parameters (water temperature, dissolved oxygen, turbidity and conductivity), bacteria during baseflow and storm conditions were compared to assess downstream changes in water quality	Cumulative impacts of other land uses appear to greatly increase turbidity, bacteria and inorganic solutes during stormflow. Likely due to overland flow and transport of materials directly to the stream
Milan Onderka & Andreas Krein	2.7 km^2 in a humid temperate catchment in Luxembourg. 98% mixed forest land cover and a network of unsealed forest roads, a primary source of sediment during runoff.	Incorporated antecedent hydro meteorological data into SSC prediction models in a headwater catchment in Huewelerbach Luxembourg. Baseflow, peak flow antecedent precipitation indices (API), total	Comparison results from 21-storm events using of a modular data driven model tree to results from conventional power-law rating curves models.	Conclusions highlight the dominant antecedent hydro-meteorological conditions acting as the major controls on the magnitude of SSC during storm events. Antecedent runoff volume explained

Authors	Study area (size)/Land Use	Data Used	Methods	Findings
		precipitation and maximum suspended sediment concentration were used. A total of 21 storm events were analyzed and API's of 1, 5,7,and 14 days were used in models		depletion of sediments
M. Seegera,*, M.-P. Erreab, S. Begueriab,	2.84 km^2 steep sloped mountainous area with bedrock of alternating sandstone and marl layers which is highly erodible and low infiltration capacity. Former land use included cereal crops that were abandoned in the middle 20th century	To understand factors leading to the Q-sed. Transport patterns. Identification of different hysteresis loops and their generation Total, average and maximum precipitation were the rainfall variables. antecedent precipitation indices (API),of 6-hours (AP6) and API's of 1,3,7,15,and 21 days were used to ,assess soil moisture conditions prior to rainfall events	Water level and suspended sediment load (measured by turbidity) and rainfall collected every 5-minutes and solar radiation, air temperature, wind speed and conductivity are measured and logged every 15-minutes.	Hysteresis loops were dependent on: Total precipitation, antecedent precipitation and soil moisture. Soil moisture was significant factor differentiating hysteretic loops. Those loops are expressions of different runoff generating processes and of changes in contributing areas
NANCY E. DRIVER and BRENT M. TROUTMAN	From a database comprised of 2,813 storms at 173 urban sites in 300 metropolitan areas throughout the U.S.	Liner regression models were developed for the estimation of storm-runoff loads and volumes from	Regional regression models were developed to relate storm-runoff loads and volumes to physical, land-use and climatic characteristics.	Total storm rainfall and total contributing drainage area most significant

		physical, land use, and climatic characteristics of urban watersheds in the US. Various chemical constituents and spatial parameters used for models		explanatory variables. Models worked best in arid states and less accurate for areas that had large quantities of mean annual rainfall

1.1 Aims and Objectives

The objective of this study is to use data collected at water-quality monitoring stations, discharge gauges and available precipitation data to identify the major hydro meteorological controls that determine the magnitude of turbidity measured in the Clackamas River during high-flow storm-runoff events. *In-situ* turbidity, acoustic and streamflow data can be used to compute a time series of suspended-sediment concentrations and loads at stream sites (Rasmussen et al., 2008). Continuous turbidity data provide a record of the changes in optical clarity of a waterbody over time and are a useful tool in efforts to study water-quality conditions, trends and other aspects concerning the dynamics and interactions within an aquatic ecosystem. Turbidity, river discharge and precipitation information will be used to understand the response of turbidity to different amounts of discharge and precipitation during high-flow storm runoff events in the Clackamas River Basin.

Understanding mechanisms controlling the transport of solids from catchments is important for maintaining high water quality and the reduction of excessive soil erosion. Adequate knowledge of sediment transport phenomena has implications for river morphology, siltation of water reservoirs, transport of sediment-bound contaminants and soil erosion (Onderka et al., 2012). In naturally vegetated headwater catchments, suspended sediments are normally transported during flood events. The use of continuous turbidity measurements can be a useful tool to assist in efforts to investigate particle transport and sediment concentrations in rivers, lakes and other water bodies.

The U.S. Geological Survey (USGS) in cooperation with the Clackamas River Water Providers (CRWP) operates a network of continuous water-quality monitors in the Clackamas Basin. These monitors measure properties of water including, water temperature, specific conductance, pH, dissolved oxygen, and turbidity. Continuous real-time data provide high-resolution information for water-quality parameters and a record of the physical changes in a waterbody over time. Information about instream processes at different times of day such as diurnal fluctuations in pH and dissolved oxygen related to algal growth, seasonal changes under various flow conditions and before/after catastrophic events such as landslides or floods. Physical properties of water, such as suspended sediments, can have substantial effects on water quality and aquatic habitat. Changes in these constituents may cause changes in other water-quality characteristics (Esralew et al., 2011).

The two sites selected for this study represent two different flow regimes in the Clackamas River drainage basin. Carter Bridge, the upper reach is located downstream of a primarily forested landscape. , and Oregon City, the lower reach, is located downstream of a mixed land-use environment. These two sites were selected for two reasons:

1. Both stations as part of the USGS gauging stations have water-quality monitors, which provide discharge and water-quality data.

2. The upper reach (Carter Bridge) and the lower reach (Oregon City) are of particular interest because they are nested. Consequently, any differences in hydrologic response to storm events can be attributed to contributions from downstream areas of the lower reach that are not included upstream of the monitoring stations on the upper reach (Sheeder et al., 2002).

In order to understand the differences in turbidity measured at these two stations, we must consider the differences in their landscape characteristics, which have a considerable amount of influence on composition of particles entering the river and being measured by the turbidity sensor; especially during storm events.

14

1.2 Research Questions –

1. Are there any differences in the mean concentration of turbidity measured during high-flow storm events between less developed upstream (the Carter Bridge) and more developed downstream (Oregon City) water-quality monitoring stations on the Clackamas River?

2. Are there any differences in the hysteresis index (HI) of turbidity between the two stations? What are the dominant hysteresis regimes in both stations by season?

3. Of the following parameters: antecedent precipitation index (API), total precipitation and discharge; which one or combinations of these parameters are the major controls that determine the change in turbidity measured during storm events in the Clackamas River?

1.3 Hypotheses

Hypothesis #1-

There are statistically significant differences in turbidity measurements during storm events between the Carter Bridge and the Oregon City water-quality monitoring stations (Figure 2).

I hypothesize that turbidity measured at each site during storm events between the two stations will be different. The Clackamas River at Carter Bridge site is the furthest upstream station and located in the predominantly forested upstream reach of the basin. The Clackamas River at Oregon City station is located in the lower reach of the basin (located at river kilometer 2.6), which is about 3% urban in comparison to only 0.4% in the upper Clackamas Basin near the Carter Bridge site (USGS, StreamStats). This study will investigate the changing turbidity during storm events between a forested rural upland sub-watershed and a downstream urban sub-watershed.

Hypothesis #2

Seasonal hysteresis patterns, as measured by hysteresis index, are expected to be different between the two sites in wet and dry seasons. I hypothesize that hysteresis patterns will show more complex pattern in the downstream site than in the upstream site. Additionally, hysteresis patterns are expected to be less pronounced in the dry season than the wet season.

Hypothesis #3-

Are stream discharge (Q), total precipitation (P_{total}) amount, antecedent precipitation indices (API) of 3, 5, 7, 14 and 30 days, or combination of these variables the major control that determines the change of turbidity during storms measured at the two selected Clackamas River sites?

I hypothesize that by using discharge, API, and P_{total} as independent variables in multiple linear regression analysis, it is possible to determine which variable (or combination of variables) correlates best with the change of turbidity measured at the two Clackamas River sites during storm events.

2. Study Area

Study Area

Located in the Cascade Range of western Oregon, the Clackamas Basin covers approximately 2,440 km^2 of forested, rural and urban land in northwestern Oregon (Figure 2). The Clackamas River originates on the western slopes of the Cascade Mountains between Mount Hood and Mount Jefferson and descends for approximately 2,190-meters on a northwesterly course winding through prominent basalt outcrops and cliffs (Carpenter, 2003). The soils in the northern part of the basin are mainly silty and many of them have a brittle hardpan in the subsoil. The soils in the southwestern portion of the basin range widely in texture and drainage, but are mostly composed of silt loam and silty clay loam (Gerig, 1985). The upper portion of the Clackamas Basin's geology and soils are primarily influenced by processes in the Cascade Mountains. In the upper portion of the basin towards the east soils are mainly well drained gravelly loam to very cobbly loam and have high content of volcanic ash, slopes are steep to very steep (Gerig, 1985). The mountains are composed of recently active volcanoes along the Cascade Crest to the east (i.e., The High Cascades), and older, inactive mountains to the west (i.e., the Western Cascades). The upper portion of the basin contains about equal portions of both of these geologic areas. The Western Cascades are steep and well-eroded with shallow subsurface confining layers, while the High Cascades form a broad volcanic platform underlain by highly porous and permeable volcanic layers (Graves and

Chang, 2007).   The upper Clackamas Basin is mostly forested and contains virtually no development aside from its road network, hydropower facilities, and a few residences (Graves and Chang, 2007).

The upstream forested areas of the basin have been affected by afforestation and deforestation (Taylor, 1999). Timber harvests in the lower basin started in the early 1800s. The lack of good roads above the Estacada area (Figure 2) and easy access to trees in the lower basin tied most activities to lower basin forests until the 1940s (Taylor, 1999).   Between 1950 and 1994 timber harvests occurred on more than 29 percent of the upper Clackamas watershed (Taylor, 1999).   Forestry operations are often associated with increased erosion. Land drainage operations, the construction of access roads and felling operations involving soil compaction and disturbance all increase erosion (Taylor, 1999).
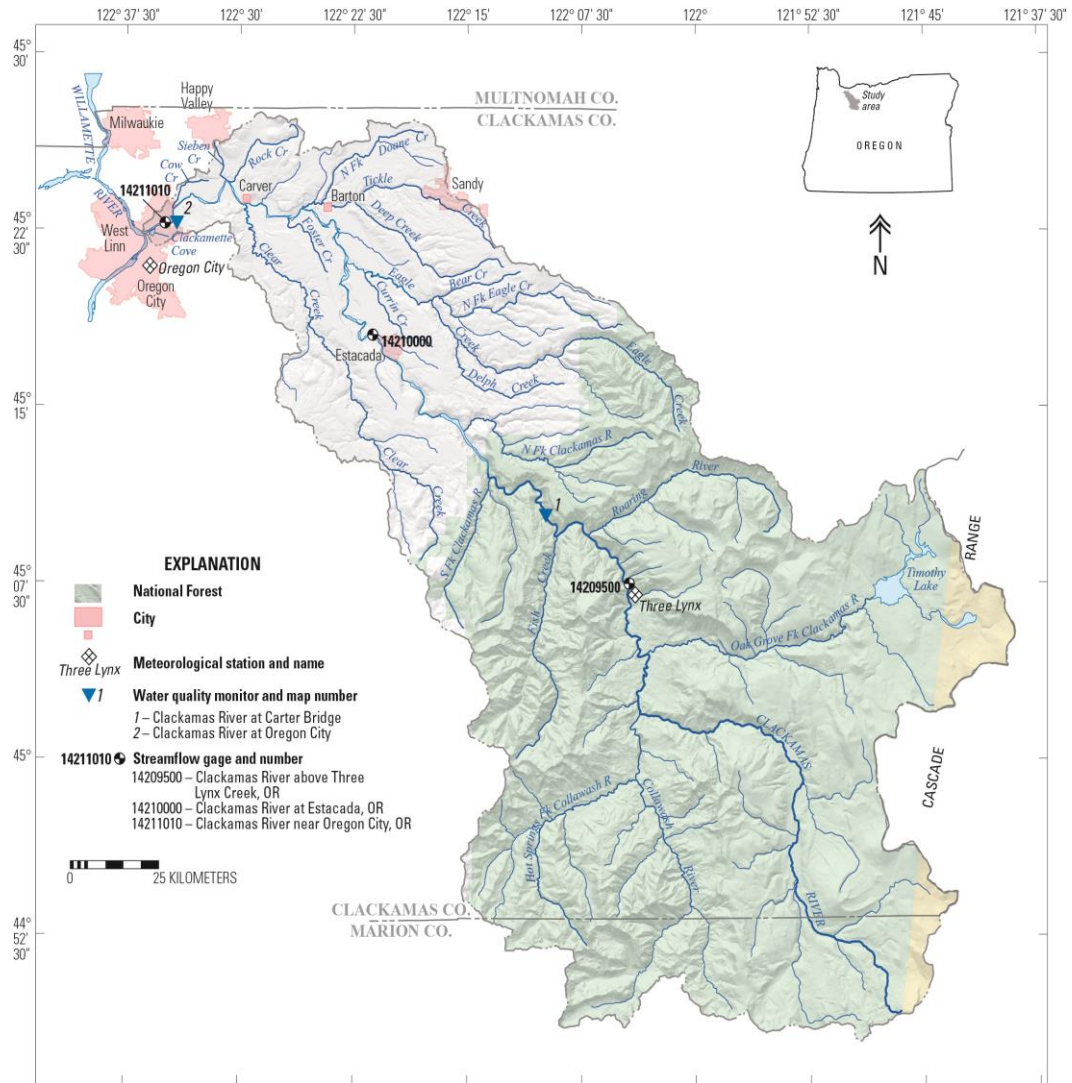
Figure 2. Map of Clackamas River Basin showing water-quality monitors, stream discharge gauging sites and precipitation stations

The Clackamas River flows for 133 kilometers from the upper-forested reaches

where it meanders through a series of tributary inputs, riffle areas and side channels

(Figure 2). The approximately 76-kilometer longitudinal distance of the Upper

Clackamas River, from its headwaters to above of North Fork Reservoir, is included as

part of the Federal Wild and Rivers System. Portland General Electric (PGE) operates three hydroelectric dams on the Clackamas River between river kilometers 75.3 and 35.9.

The Clackamas River from Carver (RK 12.9) to River Mill Dam near the Estacada gauging station (Figure 2) is a "recreational river area" under Oregon's Scenic Waterway Program (Taylor, 1999). The river also provides habitat for several migrating fish and other aquatic species. The Clackamas River supports many recreational activities, including fishing, rafting and kayaking, and it supplies drinking water for over 300,000 residents (Clackamas River Water Providers, 2017).

Downstream of Estacada, the Clackamas River widens into a lower-gradient, meandering system and is open to influences from agriculture and a growing urban population. The lower basin contains a predominantly alluvial valley, where the river flows through a broad floodplain of coarse material, much of which is mined for rock and gravel (Metro, 1997). Steep cliffs constrain the floodplain, and much of the Christmas tree and commercial tree plantations, agriculture, and rural residential areas are located on plateaus and terraces well above the floodplain. Other agricultural crops grown in the Clackamas Basin are red raspberries, strawberries, grass seed, hay along with some pasture and grazing (Gerig, 1985). Soil is susceptible to compaction if grazing is permitted when the soils are wet (Gerig, 1985). Compaction increases runoff and erosion during rain events.

Human activities in the basin, including timber harvesting, construction of roads and urban developments, farming, gravel mining, and hydroelectric power generation also may affect water quality. The largest inputs of contaminants introduced by human development occur in the lower basin, particularly on the north side of the Clackamas River, where agriculture and urban land is concentrated. Water-quality problems, such as high levels of turbidity, also occasionally occur from soil erosion, particularly in the upper basin where topography and geologic instability, combined with abundant winter precipitation contribute to erosion during periods of heavy runoff (Carpenter, 2003).

3. Data and Methods

3.1 Data

3.1.1 Turbidity Data

To obtain a minimum of 30 storm events for analysis, real-time continuous turbidity data measured in water years 2006-2012 on the Clackamas River at Carter Bridge and at the Clackamas River at Oregon City sites were used for this research. The location of the USGS water-quality monitoring (WQM) stations used for this study are listed below in Table 2 and shown in Figure 2. Mean, median and maximum daily values were computed from instantaneous data collected in 30-minute intervals by continuous water-quality monitors over the period of a day.

Turbidity measurements in the Clackamas River were obtained using a Yellow Springs Instrument (YSI) 6026 turbidity sensor attached to a YSI multi-parameter sonde. The YSI 6026 sensor is a self-cleaning turbidity sensor with a wiper (the wiper is necessary to minimize sensor fouling) designed for long-term, *in-situ* continuous turbidity monitoring. The instrument measures turbidity with an optical sensor. Light from the near-infrared light-emitting diode (LED) enters the water-sample and light rays scatter off of water particles. The light, scattered at 90 degrees, enters a detector fiber and is measured by a photodiode (Figure 2) (YSI Inc., 2009).

Table 2. Latitude and Longitude coordinates of water quality (including turbidity), discharge monitoring stations and precipitation measuring stations

Name and USGS Site Identification number	Data Collected	Latitude	Longitude
Clackamas above Three Lynx (14209500)	Discharge	45°07'30"	122°04'20"
Clackamas at Carter Bridge (14209710)	Water-quality	45°10'02"	122°09'18"
Clackamas at Oregon City (14211010)	Water-quality and Discharge	45°22'46"	122°34'34"
Three Lynx 358466-4	Precipitation	45°07'	122°04'
Oregon City 356334-2	Precipitation	45°21'	122°36'

The sensor uses a LED with a wavelength of 840 ±60 nanometers, and the detector is at an angle of 90 ±2.5 degrees to the incident light beam. Turbidity measurements obtained with these specifications are measured in Formazin Nephelometric Units (FNU). Therefore, measurements of turbidity for this study will be reported in FNU. This method conforms to the International Standardization Organization (ISO) Method 7027 of turbidity measurement (International Organization for Standardization, 1999). The strengths of ISO Method 7027 include the use of a near-monochromatic light source that is stable, low absorbance interference with samples, in low stray light (Sadar, 1999). Turbidity data used for this study have been collected, checked and reviewed in

accordance with established USGS protocols (Wagner et al., 2006). Water-quality data

from 2006–2012 selected for this study were downloaded from the USGS Data Grapher

webpage (http://or.water.usgs.gov/cgi-bin/grapher/graph_setup.pl). Summary and

statistical information for turbidity data are listed in Appendix A.
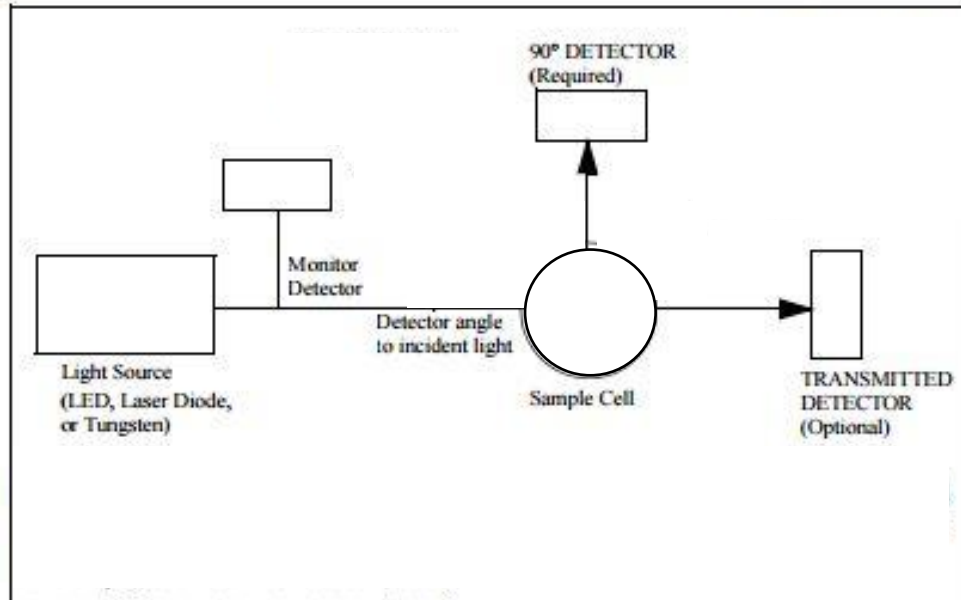
Figure 3.   Schematic of how turbidity sensor operates

3.1.2 Discharge Data

Discharge monitoring stations in the Clackamas River above Three Lynx and

Clackamas River at Oregon City were used for this study (Table 2 and Figure 2).

Streamflow discharge at these stations are measured and logged continuously every 30-

minutes. Mean daily values are calculated from the continuously logged readings.

Streamflow discharge data are collected and reviewed in accordance with USGS

protocols (Rantz et al., 1982).

25

Data from Clackamas above Three Lynx were used as a surrogate for discharge at
the Clackamas at Carter Bridge site, because Carter Bridge does not have a gauging
station. The two locations have similar basin characteristics (see Table 3). The Three
Lynx location provides suitable representation of discharge occurring downstream at
Carter Bridge, which has a drainage basin area that is roughly 20% larger than Three
Lynx. Table 3 shows a comparison of basin characteristics that demonstrate the
landscape similarity between the two sites. Summary and statistical information of
discharge data are listed in Appendix A.

Table 3. **Comparison of basin characteristics between Clackamas above Three Lynx and Clackamas at Carter Bridge sites**

Metric	Clackamas at Carter Bridge	Clackamas at Oregon City
Drainage Basin Area	1,274 km^2	1,538 km^2
Drainage Density	1.9 km^2	1.9 km^2
Mean Basin Slope	14.1 Degrees	15.5 Degrees
Total Length of Mapped Streams in Basin	932 km	1,106 km
Mean Annual Precipitation	185.4 cm	190 cm
Percentage of Impervious Area	0.023%	0.019%
Percent Forest Area	89.9%	87.8%
Percent Urban Area	0.39%	0.39%

km=kilometers, km^2= square kilometers, cm=centimeters*Data obtained from U.S. Geological Survey, 2016, The StreamStats program (USGS, 2016), which incorporates National Land Cover Database data from NLCD 2011

3.1.3 Precipitation Data

Daily point station regional precipitation data were obtained from the National Climate Data Center (NCDC), Carbon Dioxide Information Analysis Center (CDIAC) and Oak Ridge National Laboratory, Oak Ridge, Tennessee website (Menne et Al., 2013). Precipitation data collected by the NCDC are part of the United States Historical Climatology Network (USHCN) and a subset of the U.S. Cooperative Observer Network operated by the National Oceanographic Atmospheric Administration (NOAA) and National Weather Service (NWS). Location of daily precipitation stations are shown in Figure 2. Data were downloaded from the NCDC website (http://www.usclimatedata.com/climate/portland/oregon/united-states/usor0275). Summary statistics and cumulative water-year data for precipitation totals at these stations are listed in Appendix B.

3.1.4 Clackamas Basin Land Cover Data

Land cover upstream of Clackamas Basin at Carter Bridge (Figure 2) encompasses roughly 1,540 km^2 (about 63%) of the Clackamas River Basin. The Oregon City reach (Figure 2) comprises 2,437 km^2, this lower portion of the reach flows through

agricultural lands and densely-populated areas, land cover classifications for the basin

are listed in Table 3.

Table 4.   **Land Cover Information for Carter Bridge and Oregon City Watersheds**

Metric	Clackamas at Carter Bridge	Clackamas at Oregon City
Drainage Basin Area	1,538 km^2	2,437 km^2
Drainage Density	1.9 km/km^2	1.9 km/km^2
Mean Basin Slope	15.5 Degrees	4.21 Degrees
Total Length of Mapped	1,106 km	1,803 km
Mean Annual Precipitation	190 cm	185 cm
Percentage of Impervious	0.02%	1.3%
Percent Forest and Shrub land Area	98%	86%
Percent Agricultural	0%	7.0%
Percent Urban Area	0.39%	3.0%
Percent Herbaceous	1%	3.0%

km=kilometers, km^2= square kilometers, cm=centimeters

*Data obtained from U.S. Geological Survey, 2016, The StreamStats program (USGS, 2016), which incorporates National Land Cover Database data from NLCD 2011

Methods

3.1 Wet Season and Dry Season Period Delineation

    To account for seasonal variability, stream flow data collected were separated by dividing the water year (from October 1 to September 30) into two separate 6-month periods; the "wet season" (October-March) and the "dry season" (April-September). This is a typical division of seasons in marine west-coast climates (Cannon and Whitfield, 2001). A hyetograph of mean monthly precipitation totals measured at the Clackamas above Three Lynx precipitation station for the period of study are shown in Figure 3. Monthly totals were used to determine storm categorization as occurring in the wet or dry season.

    The Köppen Climate Classification System, the most widely-used system for classifying the world's climates, describes the climate in the Pacific Northwest as a Mediterranean climate. Its categories are based on the annual and monthly averages of temperature and precipitation. Mediterranean climates receive rain primarily during the winter season from mid-latitude cyclones. Extreme summer aridity is caused by the sinking air of the subtropical highs and may exist for up to 5 months (Pidwirny, 2006).

    Weather patterns in Northwest Oregon, west of the Cascades, are characterized by a mild climate, with moderate but near-continuous winter rainfall, dry summers, seasonal snowfall in the higher elevations and occasional low-elevation snowfall.

Normal winter temperature lows are often in the 20s Fahrenheit (around -6 to -7

degrees Celsius), but average in the mid 30s Fahrenheit (around 0 degrees Celsius).

Mean monthly rainfall amounts measured at Clackamas above Three Lynx,

Oregon Precipitation Station from water years 2006-2012 (Figure 3) are provided as

evidence to support the decision of the months selected to delineate the Wet Season

and Dry Season; the monthly totals are also tabled in Appendix B.

Appendix C lists the summary and statistical information of wet and dry season turbidity

and discharge data.
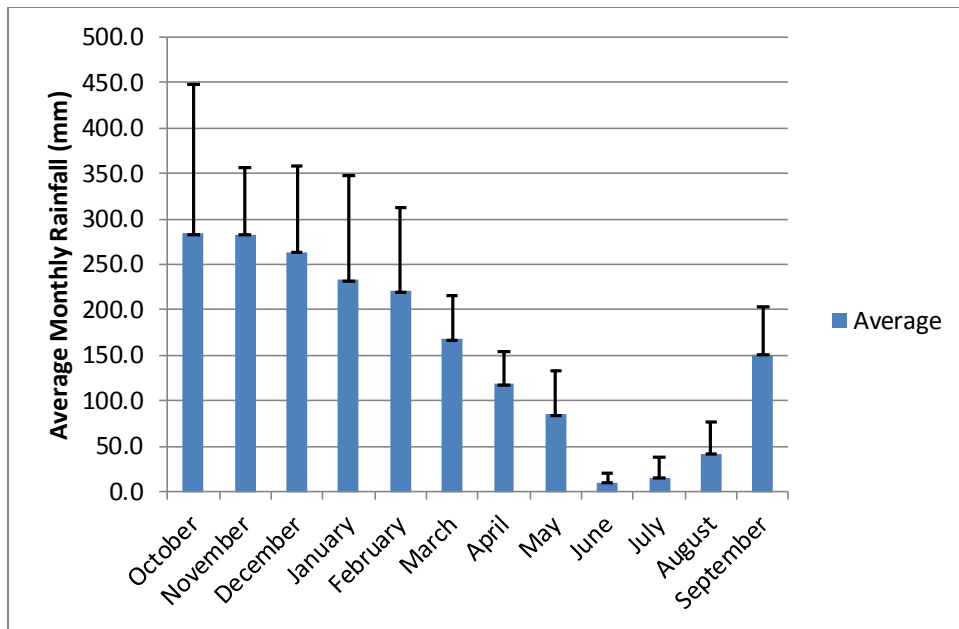
Figure 4.   Hyetograph showing monthly average rainfall amount and standard deviation for water years 2006-2012 measured at Clackamas above Three Lynx, Oregon Precipitation Station, (Data from National Climate Data Center (NCDC), Carbon Dioxide Information Analysis Center (CDIAC) and Oak Ridge National Laboratory, Oak Ridge, Tennessee), mm=millimeters

3.2.2 Storm Selection and Identification

A total of 41 storm events occurring in water years 2006 to 2012 were selected for analysis. Of these 41 events, 33 occurred during the wet season (October – March) and eight occurred during the dry season (April – September). Storms were selected using the following criteria (Figure 5):

1. A period of baseflow preceding the rising limb of the hydrograph
2. An recognizable peak discharge in the storm hydrograph
3. A return to baseflow condition following the storm event

Baseflow separation techniques using the U.S. Geological Survey PART program (Rutledge, 1993), were used to determine periods of baseflow preceding and following each selected storm event. The program PART uses streamflow partitioning to estimate a daily record of base flow under the streamflow record. The method designates baseflow to be equal to streamflow on days that fit a requirement of antecedent recession, linearly interpolates base flow for other days, and is applied to a long period of record to obtain an estimate of the mean rate of ground-water discharge (Ruthledge, 1993). PART was compared to six other baseflow separation techniques using data from 65 North American catchments (Eckhardt, 2008). Mean baseflow indices (BFI) ranged from 0.49 to 0.70 (PART BFI= 0.69), correlation between the different sets of BFI values ranged from 0.85 to 1.00 (PART=0.96) and standard

deviations (SD) ranged from 0.10 to 0.18, with SD for PART being 0.18 (Eckhardt, 2008).   A fundamental problem is that the true BFI are unknown, but for purposes of this study PART is a suitable method for determining periods of baseflow before and after storm events in the Clackamas Basin.
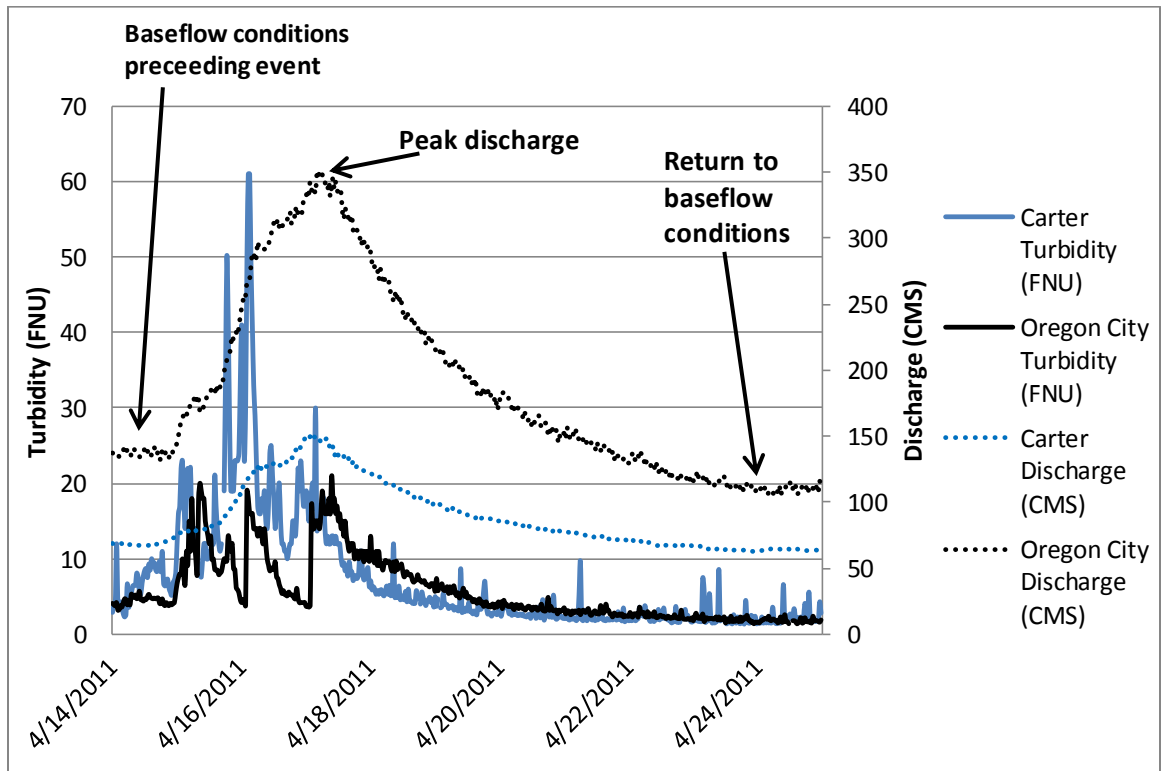
Figure 5.   An example of a storm hydrograph and turbidity at Carter Bridge and Oregon City showing baseflow preceding and following a storm event.

Storms are identified by the water year (WY) and sequentially in the order that they occur during the WY. For example, the first storm in WY 2006 is named "2006.1" and the third storm in WY 2012 is identified as "2012.3".   Storm identification and dates

of each event for Carter Bridge and Oregon City are listed in Appendix D. Figure 6 is an

example of a storm event hydrograph occurring in late January to early-February 2012,

showing discharge and turbidity measured at both the Carter Bridge and Oregon City

sites.
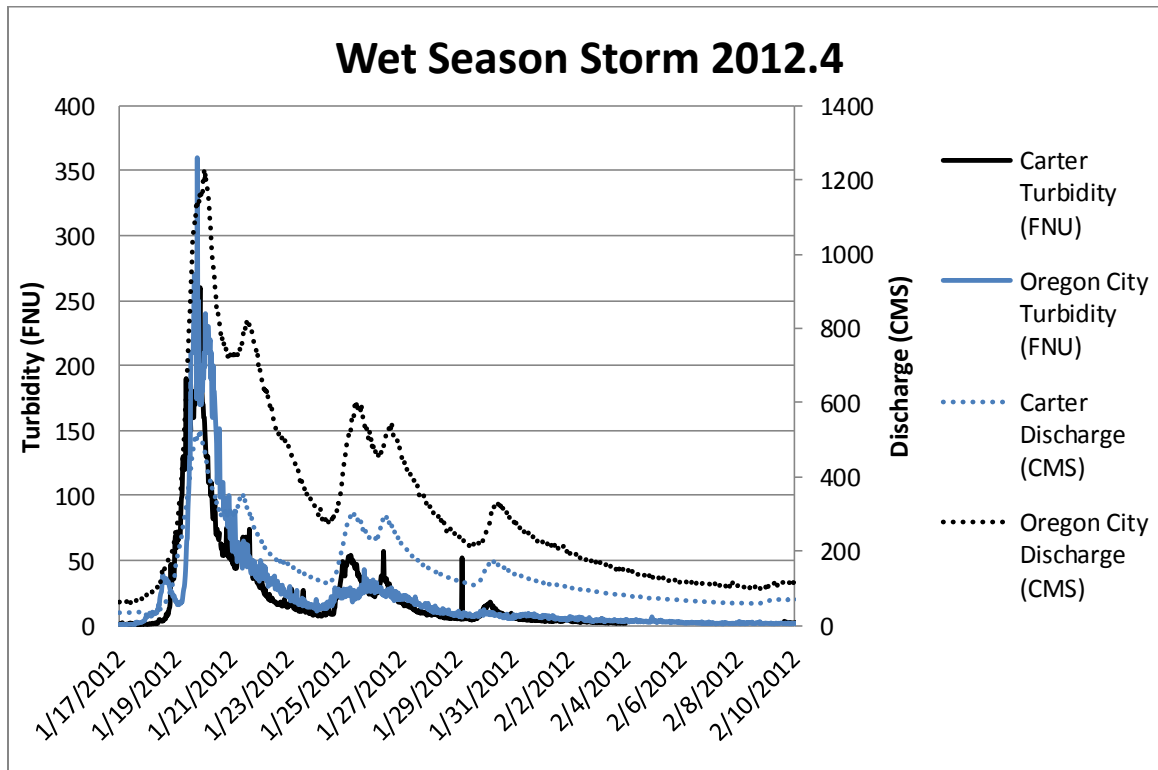
Figure 6.   Example of "Wet Season Storm 2012.4" storm events hydrograph and turbidity graphs. FNU=Formazin Nephelometric Units, CMS=cubic meters per second

3.2.3 Hysteresis Index

A hysteresis index (HI) was used to quantify the magnitude and direction of the hysteretic effect present in the discharge and turbidity relationship. The HI compares the turbidity values measured at the midpoint of discharge of the rising and falling limbs of the storm event hydrograph (Lawler et al., 2006). The HI assigns a positive direction for clockwise hysteresis (C), when turbidity is higher at the midpoint on the rising limb of the storm hydrograph than on the falling (recession) limb at the same discharge and assigns a negative value for counterclockwise (CC) hysteresis when the opposite is true. When no hysteresis is present, HI is given a zero value. HI standardizes a specific discharge at the midpoint of the storm hydrograph on the rising and falling limbs and expresses the magnitude and direction of the hysteresis symmetrically in a single number. The HI index is also used to assess whether or not seasonal differences exist between the storm responses at the two stations. The midpoint of discharge was calculated using the following equation:

$$Q_{mid} = k(Q_{max} - Q_{min}) + Q_{min} \tag{1}$$

where Q_{mid} is the discharge at the midpoint between Q_{max}, the peak discharge during the event, and Q_{min}, the discharge prior to the rise in the hydrograph preceding the event. The k value (0.5) represents the position at which the hysteresis loop is assessed in relation to discharge during the event. Figure 6 depicts a representation of the points on a storm hydrograph and turbidity graph that are used to calculate HI. Turbidity values measured at these specific discharges were used to calculate the HI. The two turbidity values at Q_{mid} called TU_{RL} on the rising limb of the hydrograph and TU_{FL}, the turbidity

value associated with Q_{mid} on the falling limb of the hydrograph are interpolated and

HI_{mid} calculated as:

For clockwise hysteresis (Figure 7) where:

$TU_{RL} > TU_{FL}$, HImid = (TU_{RL}/ TU_{FL}) -1   (2)

For counterclockwise hysteresis where:

$TU_{RL} < TU_{FL}$, HImid = $(-1 / TU_{RL}/ TU_{FL})) +1$ (3)

this method was utilized to investigate turbidity dynamics in an urban stream in the

United Kingdom by Lawler and others, 2006.
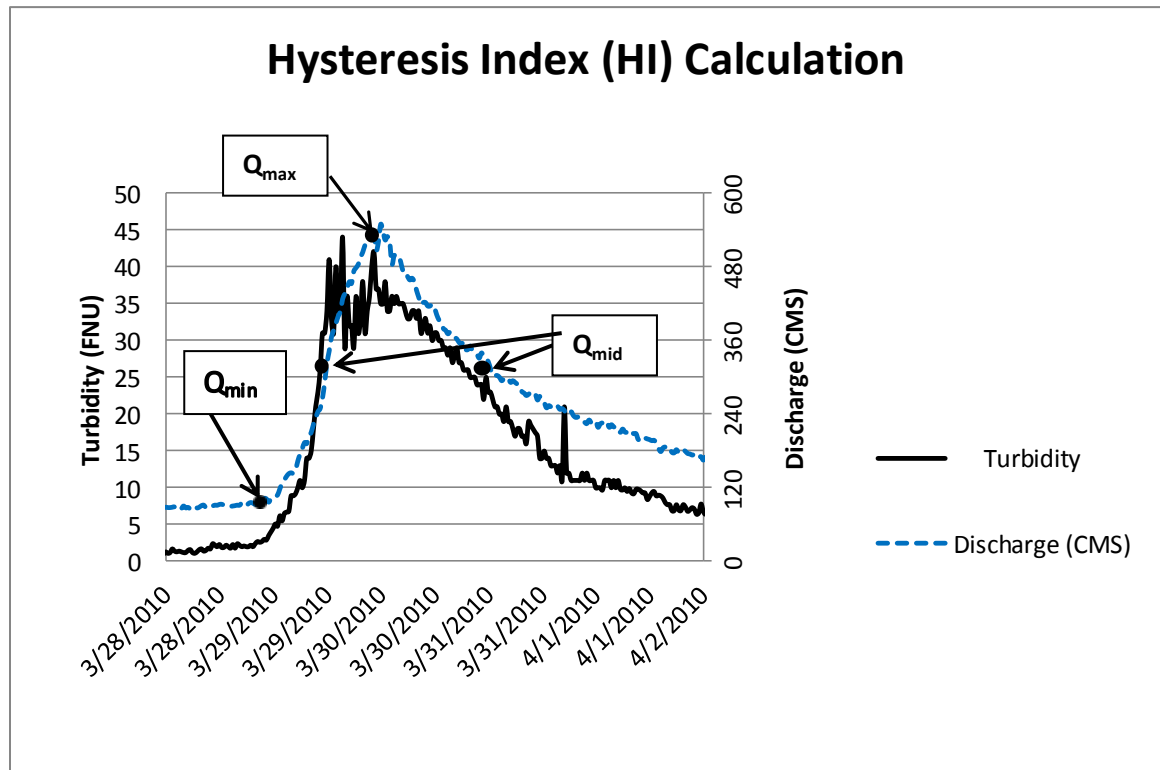
Figure 7.   Example diagram using data from storm event at Oregon City occurring from 3/38/2010 to 4/2/2010 (event # 2010.4), showing points on hydrograph where concurrent turbidity values measured at specific discharges points during an event were used to calculate a hysteresis index (HI). Qmin =the discharge prior to the rise in the hydrograph preceding the event; Qmid = the discharge at the midpoint between , Qmin and Qmax = the peak discharge during the event; FNU=Formazin Nephelometric Units; CMS=cubic meters per second

Figure originally from Lawler, 2006
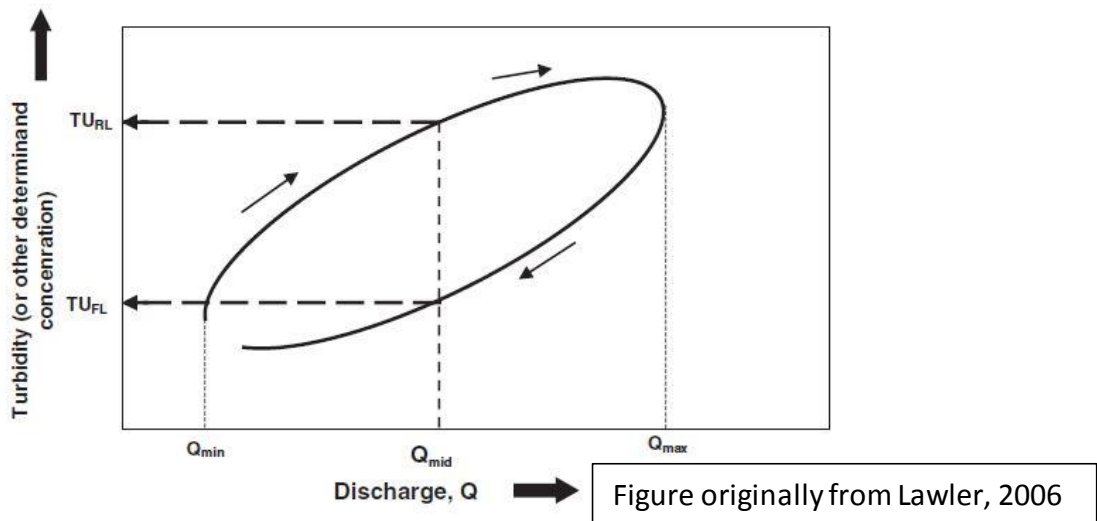
Figure 8.   Schematic diagram depicting clockwise hysteresis using equations 1 and 2. TURL =Turbidity on the rising limb of the hydrograph, TU FL = Turbidity on the falling limb of the hydrograph Qmin =the discharge prior to the rise in the hydrograph preceding the event, Qmid =the discharge at the midpoint between , Qmin= prior to the beginning of the rise in the hydrograph, Qmax=the peak discharge during the event

3.2.4 Antecedent Hydro-meteorological Conditions

Precipitation amount and soil moisture are important controlling factors for

storm runoff amounts (Sun et al., 2002).   The antecedent precipitation index (API) was

used to account for a composite measure of water storage in the basin including

36

depression storage, surface water conditions and also as a way to gage soil moisture conditions prior to a rainfall runoff event. Several researchers have used API as a variable in rainfall runoff models and other studies as a method to describe soil moisture conditions (Fedora and Beschta, 1989, Ali et. al, 2010, Onderka et.al, 2012). API was calculated for 3, 5, 7, 14, and 30 days as:

$$\text{API}_n = \sum_i^n Pi \qquad\qquad (4)$$

Where *n* is the number of days for which API is calculated starting from the day of an event and *Pi* in millimeters per day is the total precipitation on the *i* th day before the event. These API indices were selected in effort to test a range of API values to represent soil moisture conditions for use in the multiple linear regression analysis.

3.2.5 GIS Land Cover Data Analysis along River Channel

GIS analysis was used to identify land cover type within a 100 and 200-meters of the main Clackamas River channel. This was done to categorize the land use of the riparian zone near the Carter Bridge and Oregon City water quality monitoring stations. Land cover classification data near the riparian zone will provide additional information that could further explain differences in turbidity due to runoff during storms between the two stations. The 2011 National Land Cover Database (NLCD) was used for this analysis. The NLCD provides spatial reference and descriptive data for characteristics of the land surface (Homer et al., 2012).

The following methods were used calculate land cover near the main stem Clackamas River to create 100 and 200-meter buffers of the Clackamas River:

1. The USGS StreamStats basin delineation tool was used to create shape files of the watersheds upstream of each site.

2. A 2011 NLCD Land Cover of the State of Oregon that also contained National Hydrologic Dataset (NHD) Layer the was obtained from USGS data base

3. The "Clip" tool in Arc GIS (version 10.4.1) was used to "Clip" the shape files delineating the Clackamas Basin

4. The Clackamas River was selected from the Attribute Table and 100 and 200 meter buffers were created using the "Buffer" tool

5. The "Tabulate Area" function was then used to calculate land cover types within each of the buffers

6. "dbf" files created where then opened in Excel to tabulate the calculated land cover areas.

Land cover type within the selected buffer distances were calculated to characterize land-use near each turbidity monitoring site

3.2.6 Statistical Analysis

Paired t-test

A paired t-test comparing HI values between storm events at the Carter Bridge and Oregon City sites was performed using the R statistical software (version 3.0.2). The paired t-test was used to test the null hypothesis H_o, and the alternative hypothesis H_a:

(H_o): Calculated hysteresis index during selected storm events is the same at both sites.

(H_a): Calculated hysteresis index during selected storm events are not the same at both sites

Calculated hysteresis indexes during each storm event analyzed for this study were compared. The null hypothesis (H_0) was rejected if the p-value from the paired t-test was less than or equal to 0.05. Test statistics and results for each comparison are listed in Appendix D.

3.2.7 Shapiro-Wilk Test

The Shapiro-Wilk test was performed on turbidity and discharge values used for multiple linear regression analysis. Transformations such as logarithms are used to better meet the assumptions of parametric analysis (normality, linearity, and constant variances) and they are used as a diagnostic tool to aid in the identification of outliers

39

and extreme data points. Shapiro Wilk test values for turbidity and log transformed turbidity are listed in Appendix F. Transformed and untransformed turbidity values were compared and log transformed turbidity values were used for model development. Log transformed values better met the conditions for normality tests.

3.2.8 Regression analysis

Multiple linear regression (MLR) was used to determine which explanatory variables or combination of variables best correlate with turbidity during storm events. Variable selection was performed using backward stepwise selection. Backward stepwise linear regression in R (version 3.0.2) was used to select the best model to determine which independent variable or group of variables best explain turbidity response during storm events. Linear regression models were developed that related the change in turbidity during storm events to measurable physical conditions and meteorological parameters. When evaluating the importance of a set of independent variables for prediction of a dependent variable, a stepwise technique is important in exploring behavior in a process-response model. Any attempt to develop a model of this form is limited by implicit assumptions of data normality, problems of multi-collinearity amongst the independent variables and serial correlation in the residuals (Foster, 1978). Independent variables used for developing the models are listed below in Table 5, and data table matrices used for Carter Bridge and Oregon City multiple linear regression models are shown in Appendix G.

Model selection was performed in R which uses Akaike Information Criteria (AIC) as a best-fit measure for model selection. The following hydrological and meteorological variables were used as independent variables:

1. Change in stream flow (ΔQ)

2. 3, 5, 7, 14, 30-day antecedent precipitation index (API#)

3. Total precipitation (P) amounts measured during storms events

Table 5.   Independent variables used for model development

Parameter	Symbol	Unit of Measure
Change in Discharge	(ΔQ)	cubic meters per second (m^3/sec)
Total Precipitation	P	mm (total)
3-Day antecedent precipitation	API3	mm (total)
5-Day antecedent precipitation	API5	mm (total)
7-Day antecedent precipitation	API7	mm (total)
14-Day antecedent precipitation	API14	mm (total)
30-Day antecedent precipitation	API30	mm (total)

The combination of variables (or variable) that provides the "best fit" in the regression analysis will be considered the major hydrological and meteorological control best determines turbidity during storm events.

3.2.9 Model Diagnostics

A number of graphical and statistical tools were used to examine the results of regression models. Leverage is a measure of an "outlier" in the x direction. It is a function of the distance from the ith x value to the middle (mean) of the x values used in the regression (Helsel, 2002). The Durbin Watson and Bruessch-Godfrey tests were performed on the final models to check for serial autocorrelation of the residuals. In

regression analysis, variance may be biased because of dependence of the error residuals as a result of serial autocorrelation (Helsel and Hirsch, 2002). Serial autocorrelation is correlation between a data point and its adjacent points in a time series (Helsel and Hirsch, 2002).

Another model diagnostic tool is Cook's distance. Cook's distance measures the effect of a particular data point. Points with a large Cook's distance should be examined closely and considered for deletion. When cases are outside of the Cook's distance they are influential to the regression results. The regression results are altered if we exclude those cases. The Durbin Watson and Bruesch-Godfrey tests were performed on the final models to check for serial autocorrelation of the residuals.

4. Results

4.1 Summary of Turbidity Data

In water years (WY) 2006-2012 the mean daily turbidity at Carter Bridge was 5.1 FNU, and the mean daily turbidity at Oregon City was 4.5 FNU with a standard deviation of 18.5 and 14.2, respectively. Median turbidity at Carter Bridge and Oregon City was 1.5 FNU and 1.4 FNU, respectively with an inter-quartile range of 2.7 FNU at both sites. Minimum daily turbidity during the study period was 0 FNU at both sites, and the maximum daily turbidity during the study period at both sites was 340 FNU. Figure 8 illustrates the range of log turbidity values at Carter Bridge and Oregon City during water years 2006-2012. Turbidity values were log transformed for improved visual comparison. Summary statistics of turbidity values during the study period are in Appendix A.
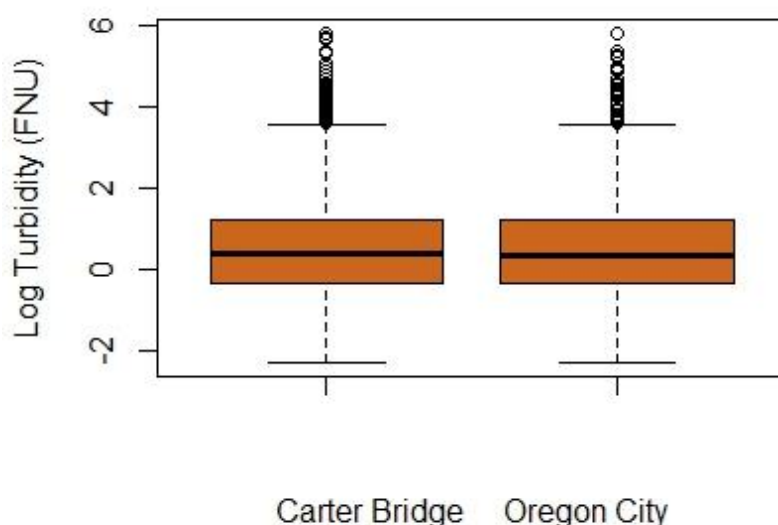
Figure 9.   Boxplot Comparison of Mean Daily Log Turbidity at Carter Bridge and Oregon City for Study Period (n =41)

In water years (WY) 2006-2012 the mean daily turbidity at Carter Bridge and Oregon City during the "Wet Season" was 8.2 FNU and the mean daily turbidity at Oregon City was 7.3 FNU, with a standard deviation of 22.6 and 19.5 respectively. Median turbidity at Carter Bridge and Oregon City was 2.2 FNU and 2.4 FNU, respectively with an inter-quartile range of 4.0 FNU at Carter Bridge and 5.0 at Oregon City. Minimum daily "Wet Season" turbidity during the study period was 0.0 FNU at both sites. The maximum daily turbidity during the "Wet Season" was 340 FNU at both sites. Figure 9 is a boxplot comparing turbidity at both sites during the "Wet Season" of water years 2006-2012.   Turbidity values were log transformed to aide comparison. Summary

statistics of turbidity "Wet and Dry Season" turbidity during the study period are shown

in Appendix C.
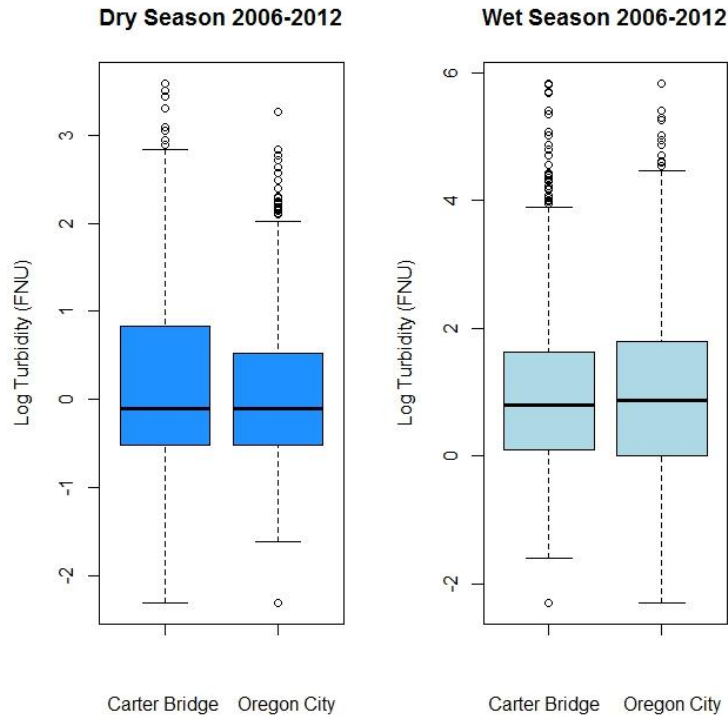
Figure 10. Boxplots showing log transformed mean daily turbidity measured at Carter Bridge and Oregon City during the Wet and Dry Season in water years 2006-2012

In water years WY 2006-2012 the mean daily turbidity during the "Dry Season"

at Carter Bridge was 2.0 FNU and at Oregon City it was 1.6 FNU with a standard

deviation of 3.1 and 2.1, respectively. Median turbidity at both sites was 0.9 FNU, with

an inter-quartile range of 1.7 at Carter Bridge and 1.1 at Oregon City. Minimum daily

turbidity during the study period was 0.0 FNU at both sites. The maximum daily turbidity

during the "Dry Season" was 36 FNU at Carter Bridge and 26 FNU at Oregon City. Figure

10 illustrates an intrasite comparison of log transformed "Wet and Dry Season" turbidity at Carter Bridge and Oregon City during WY 2006-2012. Turbidity values were log transformed to aide comparison. Summary statistics of turbidity "Wet and Dry Season" turbidity during the study period are in shown in Appendix C.
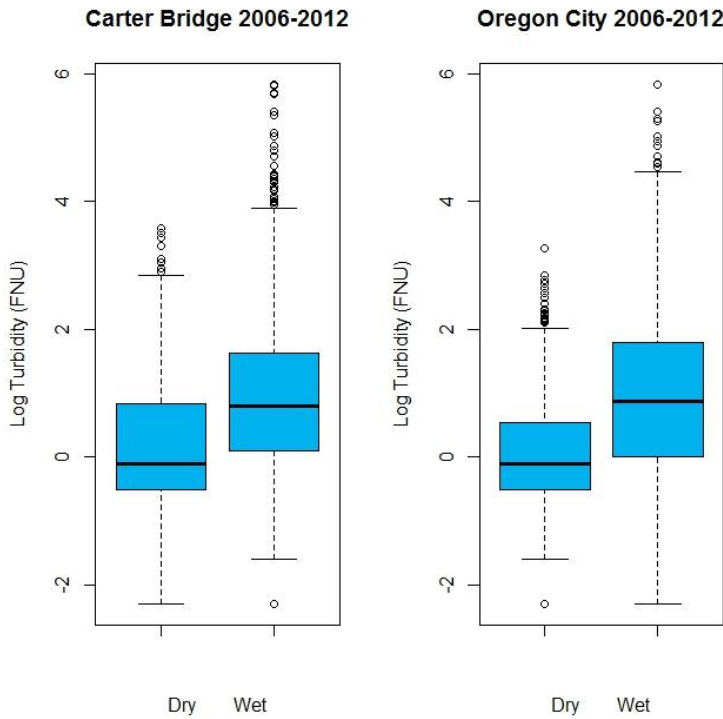
Figure 11.   Intrasite comparison of Turbidity in Wet and Dry Seasons from 2006-2012 at Carter Bridge and Oregon City

Turbidity values measured during the "Wet Season" were higher than those measured in the "Dry Season" at both sites.

47

4.2 Hysteresis Index by season and site

The Carter Bridge site exhibited clockwise (C) hysteresis index (HI) in 38 of the 41 storm events (92.6% of the time) and counter clockwise (CC) HI value in 3 events. The mean HI value for all storms at Carter Bridge was 1.86; the median HI value was 1.43 with a standard deviation of 2.25. HI values ranged from -2.25 to 9.00. The lowest HI value occurred during storm 2006.8 from March 7, 2006 to March 12, 2009. The highest HI value occurred during storm 2006.7 from February 27, 2006 to March 5, 2006.

The Oregon City site exhibited clockwise hysteresis in 29 of the 41 storms (73.1% of the time); counter clockwise in 11 and one storm's calculated HI was "0". The mean HI value for all storms at Oregon City was 0.96; the median HI value was 0.39 with a standard deviation of 1.95. HI values ranged from -2.04 to 8.06. The lowest HI value occurred during storm 2009.5 from May 4, 2009 to May 22, 2009. The highest HI value occurred during storm 2007.1 from October 31, 2006 to November 12, 2006.

HI values for the Carter Bridge and Oregon City and the data used to compute the values are shown in Appendix E.

The Carter Bridge site (n=41) had a mean HI of "1.86" and a standard deviation (SD) of "2.25". By comparison Oregon City (n=41) had a numerically smaller mean HI value of "0.96" (almost half) and a SD of "1.95". To test the hypothesis that HI values calculated for storms at Carter Bridge and Oregon City were associated with statistically significant different HI values a two-sided t-test was performed. Results are shown in Table 5. The

assumption of equal variance was tested and satisfied via a Levene's F test, df (39) = 1.17, p-value = 0.632, results are shown in Table 6. The two-sided t-test was associated with a statistically significant effect, df (39) = 1.81, p = 0.078. Thus Carter Bridge HI values were associated with a statistically significant larger HI than Oregon City. Box and whisker plots of calculated HI values are shown in Figure 11.

Table 6.   **Statistical Summary of Hysteresis Indices Calculated at Study Sites**

Site	Hysteresis Index (HI) Values Compared (N)	Degrees of Freedom (df)	Mean Hysteresis Index (HI)	Standard Deviation (SD)	Interquartile Range (IQR)
Carter Bridge	41	39	1.86	2.25	2.05
Oregon City	41	39	0.96	1.95	2.19

Table 7.   **Results of Two-sided t-Test and Levene's F-Test of Hysteresis Indices**

Statistical Test	Test Value	Degrees of Freedom (df)	p-value
Two-sided t-Test	1.81	39	0.078
Levene's F-Test	1.17	39	0.632
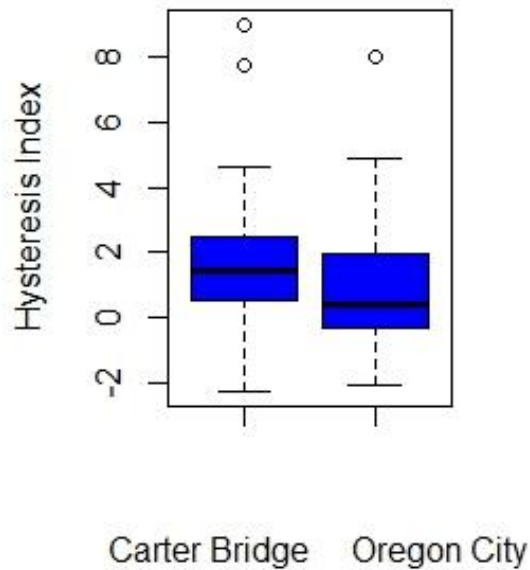
Figure 12. Boxplot of Calculated HI Values from Clackamas River at Carter Bridge and Clackamas at Oregon City (n = 41)

Land Cover Characterization within 100 and 200 Meter Buffer Zones of Clackamas River

The majority of land cover within both the 100 and 200-meter buffers for both sites was forest land (combined deciduous, evergreen and mixed) and shrub-scrub types, with Carter Bridge having slightly over 85% and Oregon City having 59.3% forested land cover in the 100-meter buffer. Carter Bridge is classified as 85% forest and shrub-scrub land cover and Oregon City classified as having 65.9% within the 200-meter buffer zone.

The Carter Bridge site has about 0.3% developed land of (combined low, medium and high) and Oregon City has about 2.7% developed land in the 100-meter buffer, which is roughly an order of magnitude greater by comparison. The Carter Bridge site has slightly over 0.2 % developed land (combined low, medium and high) and Oregon City has about 4.0% developed land in the 200-meter buffer, which is about double an order of magnitude distinction by comparison. The Carter Bridge buffers have no agricultural or wetland land cover, however and Oregon City has about 1.5% agricultural and 7.6% wetland land cover within the 100-meter buffer zone and 3.0% agricultural and 5.9% wetland land cover within the 200-meter buffer. Numerically the differences in land cover within the 100 and 200-meter buffers for developed, agricultural land and wetland may not appear to be very substantial; however this difference represents a potential contrast in sediment and particulate matter available to be entrained into the river channel during storm events. Table 4 lists land cover classification percentages within the 100 and 200 meter buffers at both sites.

Table 8. Percentage of Land Cover Classifications within 100-meter and 200-meter Buffer Regions of the Clackamas River at Carter Bridge and Oregon City based on 2011 National Land Cover Data (NLDC)

Site and Buffer Region	Open Water	Developed Open Space	Developed Land	Barren Land	Forest and Shrub Land	Grassland	Cultivated Crops and Hay	Wetlands
Carter 100-meter Buffer	4.4%	9.3%	0.3%	0.4%	85.0%	0.5%	0.0%	0.0%
Oregon City 100-meter Buffer	15.0%	10.1%	2.7%	1.6%	59.3%	2.4%	1.4%	7.6%
Carter 200-meter Buffer	2.2%	8.0%	0.3%	0.3%	88.7%	0.5%	0.0%	0.0%
Oregon City 200-meter Buffer	8.7%	8.8%	4.0%	1.1%	65.9%	2.8%	3.0%	5.9%

4.3 Relation between discharge and turbidity

The best model results for Carter Bridge and Oregon City storm events were as follows:

Carter Bridge: Log ΔTurb = -2.75 + 1.24 * Log ΔQ　　　　　　(3)

Oregon City: Log ΔTurb =　-2.19 + 0.96 * Log ΔQ　　　　　　(4)

The best model results for Carter Bridge and Oregon City Wet Season storm events were as follows:

Carter Bridge: Log ΔTurb = -3.32 + 1.37 * Log ΔQ　　　　　　(5)

Oregon City: Log ΔTurb =　--1.96 + 0.95 * Log ΔQ　　　　　　(6)

The best model results for Carter Bridge and Oregon City Dry Season storm events were as follows:

Carter Bridge: Log ΔTurb = -0.57 + 0.75 * Log ΔQ　　　　　　(7)

Oregon City: Log ΔTurb =　-4.70 + 1.25 * Log ΔQ +0.03*API3　　　　　　(8)

Where Log ΔTb= Ln of the change in turbidity during the storm event, Log ΔQ= Ln of the change in discharge during the storm event and API3=3 day antecedent precipitation index
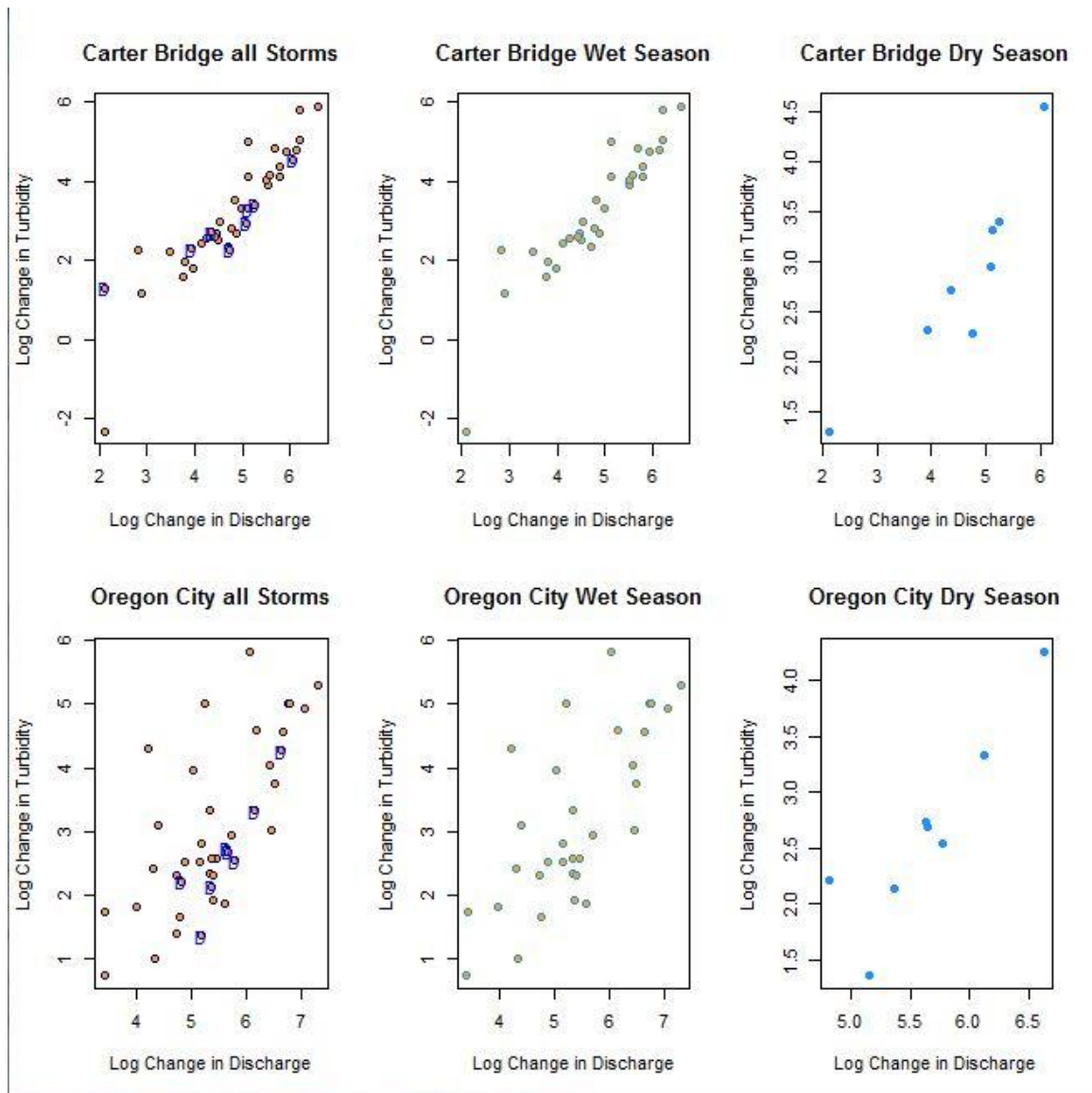
Figure 13. Scatter plots of linear fit of Log ΔTb as a function of Log ΔQ at Clackamas at Carter Bridge and Oregon City, Log ΔTurb=Natural Log (Ln) of change in turbidity from initial increase to peak value during storm event, ΔQ=Natural Log (Ln) of change in discharge from initial increase to peak value during storm event, "D" denotes dry season storm event

All variables from Table 5 were used for the stepwise regression models and "Log ΔQ" alone produced the best fit. Model summaries are listed in Table 10.

Table 9.

Data used for Carter Bridge Multiple Linear Regression Analysis-

Event	Dates	$Tb_{initial}$	Tb_{Max}	deltaT	LogDTb	$Q_{initial}$	Qmax	DeltaQ	LogDQ	$Precipitation_{Total}$
2006.1	11/10-11/24	1.8	8.9	7.1	1.96	38.8	85.8	44.7	3.80	48.3
2006.2	12/18-12/26	0.8	81.0	80.2	4.38	41.1	354.0	328.7	5.79	113.3
2006.3	12/29-1/6	45.0	160.0	115.0	4.74	224.3	560.7	376.1	5.93	188.0
2006.4	1/28-2/11	17.0	45.0	28.0	3.33	91.2	219.7	145.6	4.98	181.6
2006.5	2/27-3/5	3.2	13.0	9.8	2.28	48.1	62.6	16.7	2.82	35.3
2006.6	3/7-3/12	2.6	2.7	0.1	-2.30	51.0	57.8	8.2	2.11	61.0
2006.7	4/2 -4/30	1.9	12.0	10.1	2.31	49.8	103.6	51.5	3.94	119.4
2007.1	10/31 - 11/12	0.6	330.0	329.4	5.80	20.6	515.4	494.9	6.20	315.2
2007.2	12/8-12/22	2.1	130.0	127.9	4.85	53.0	356.8	293.1	5.68	186.2
2007.3	12/22-1/7	4.9	68.0	63.1	4.14	86.4	253.2	169.1	5.13	241.8
2007.4	3/24-4/1	2.0	8.1	6.1	1.81	69.9	122.9	53.2	3.97	60.2
2008.1	10/15-10/26	0.2	20.0	19.8	2.99	19.4	113.3	94.0	4.54	104.9
2008.2	11/15- 11/26	1.0	16.0	15.0	2.71	38.5	186.0	87.5	4.47	101.6
2008.3	12/1-12/16	0.9	120.0	119.1	4.78	34.0	501.2	466.1	6.14	162.1
2008.4	5/14-5/28	5.8	36.0	30.2	3.41	113.3	283.2	191.4	5.25	82.5
2009.1	10/27-11/5	0.5	3.8	3.3	1.19	22.5	40.8	18.2	2.90	64.5
2009.2	11/5-11/18	1.6	52.0	50.4	3.92	33.7	288.8	252.0	5.53	142.5
2009.3	12/23-1/20	0.8	150.0	149.2	5.01	29.2	194.3	167.9	5.12	326.7
2009.4	2/21-3/17	0.6	13.0	12.4	2.52	28.9	122.3	90.6	4.51	256.0
2009.5	5/4-5/31	3.4	31.0	27.6	3.32	96.8	258.0	169.9	5.14	137.9
2010.1	11/5 - 11/16	0.7	5.6	4.9	1.59	26.8	69.4	43.3	3.77	152.4
2010.2	12/9 - 12/30	0.6	17.0	16.4	2.80	25.5	145.3	119.1	4.78	182.6
2010.3	1/4 -1/15	3.4	14.0	10.6	2.36	84.1	192.8	110.7	4.71	80.5
2010.4	3/28- 4/5	2.6	59.0	56.4	4.03	56.1	303.0	247.5	5.51	148.1
2010.5	6/1 -6/22	1.8	21.0	19.2	2.95	52.4	216.6	164.5	5.10	164.6
2010.6	9/14-10/2	0.7	4.4	3.7	1.31	21.1	30.0	8.4	2.13	76.7
2011.1	10/20-10/30	0.7	10.0	9.3	2.23	18.3	55.2	32.9	3.49	108.2
2011.2	11/13-11/26	2.5	16.0	13.5	2.60	38.8	122.3	84.1	4.43	145.8
2011.3	11/26-12/7	2.4	14.0	11.6	2.45	39.6	111.0	62.0	4.13	88.9
2011.4	12/7-12/25	1.4	66.0	64.6	4.17	42.2	305.8	265.6	5.58	255.8
2011.5	12/25-1/7	3.9	17.0	13.1	2.57	51.0	121.2	70.5	4.26	91.7
2011.6	1/11-2/2	1.2	360.0	358.8	5.88	38.8	775.9	736.0	6.60	191.3
2011.7	4/14-4/24	6.8	22.0	15.2	2.72	68.8	151.8	77.6	4.35	67.8
2012.2	11/21-12/26	3.2	37.0	33.8	3.52	33.7	156.6	125.7	4.83	119.1
2012.3	12/27-1/16	1.2	120.0	118.8	4.78	23.5	481.4	458.7	6.13	229.9
2012.4	1/17-2/10	1.0	160.0	159.0	5.07	34.3	518.2	493.3	6.20	416.6
2012.5	2/17-3/3	1.3	16.0	14.7	2.69	59.2	187.5	130.5	4.87	175.0
2012.6	3/9-3/27	2.1	64.0	61.9	4.13	61.7	387.9	327.3	5.79	238.5
2012.7	3/29-4/10	15.0	110.0	95.0	4.55	101.7	512.5	430.4	6.06	134.9
2012.8	4/15-5/13	1.2	11.0	9.8	2.28	81.0	196.5	115.0	4.74	182.9

Event-storm identification, $Tb_{initial}$-turbidity at beginning of event in formazin nephelometric units (FNU), Tb_{Max}-Peak turbidity during event in formazin nephelometric units (FNU) , deltaTb-change in turbidity from initial to peak in formazin nephelometric units (FNU), , LogDTb-log of deltaT [ln(cubic meters per second)], $Q_{initial}$- discharge at beginning of event [ln(cubic meters per second)], Qmax-discharge Peak turbidity during

event[ln(cubic meters per second)] , DeltaQ-change in discharge from initial to peak[ln(cubic meters per second)] , LogDQ-log of DeltaQ[ln(cubic meters per second)] , Precipitation$_{Total}$-total precipitation during event(millimeters))

Table 10. Data used for Oregon City Multiple Linear Regression Analysis

Event	Dates	Tb$_{initial}$	Tb$_{max}$	DeltaTb	LogDTb	Q$_{initial}$	Q$_{max}$	deltaQ	LogDQ	Precipitation$_{Total}$
2006.1	11/10-11/24	1.8	7.1	5.3	1.67	69.4	186.9	117.5	4.77	38.1
2006.2	12/18-12/26	0.5	53.0	52.5	3.96	34.8	186.3	151.5	5.02	121.4
2006.3	12/29-1/6	39.0	190.0	151.0	5.02	461.6	1305.4	843.8	6.74	5.1
2006.4	1/27-2/11	8.1	30.0	21.9	3.09	136.8	218.3	81.6	4.40	13.5
2006.5	2/27-3/5	1.8	13.0	11.2	2.42	69.1	142.2	73.1	4.29	7.6
2006.6	3/7-3/12	2.9	8.6	5.7	1.74	83.3	113.8	30.6	3.42	56.1
2006.7	4/2-4/30	1.8	11.0	9.2	2.22	87.5	211.8	124.3	4.82	70.4
2007.1	10/31 - 11/12	0.9	150.0	149.1	5.00	25.8	211.8	186.0	5.23	187.0
2007.2	12/8-12/22	0.5	100.0	99.5	4.60	85.2	557.8	472.6	6.16	15.0
2007.3	12/22-1/7	6.4	80.0	73.6	4.30	151.5	219.5	68.0	4.22	32.8
2007.4	3/24-4/1	1.4	18.0	16.6	2.81	111.6	286.0	174.4	5.16	15.7
2008.1	10/15-10/26	0.5	13.0	12.5	2.53	30.3	162.3	132.0	4.88	105.4
2008.2	11/15- 11/26	0.7	14.0	13.3	2.59	54.7	288.8	234.2	5.46	108.7
2008.3	12/1-12/16	2.8	98.0	95.2	4.56	72.2	841.0	768.8	6.64	100.8
2008.4	5/14-5/28	0.6	16.0	15.4	2.73	158.9	436.1	277.2	5.62	49.0
2009.1	10/27-11/5	0.4	6.6	6.2	1.82	26.5	80.1	53.7	3.98	63.0
2009.2	11/5-11/18	2.7	23.0	20.3	3.01	58.1	688.1	630.0	6.45	117.9
2009.3	12/23-1/20	0.9	340.0	339.1	5.83	43.3	464.4	421.1	6.04	193.3
2009.4	2/21-3/17	0.5	11.0	10.5	2.35	47.6	252.3	204.7	5.32	144.5
2009.5	5/4-5/31	2.3	17.0	14.7	2.69	153.8	436.1	282.3	5.64	17.5
2010.1	11/5 - 11/16	1.0	11.0	10.0	2.30	39.1	152.6	113.5	4.73	97.3
2010.2	12/9 - 12/30	0.7	14.0	13.3	2.59	36.5	245.2	208.7	5.34	112.0
2010.3	1/4 -1/15	4.2	11.0	6.8	1.92	148.4	365.3	216.9	5.38	60.9
2010.4	3/28- 4/5	2.0	30.0	28.0	3.33	91.8	549.3	457.6	6.13	110.5
2010.5	6/1 -6/22	2.3	15.0	12.7	2.54	116.4	438.9	322.5	5.78	94.5
2010.6	9/14-10/2	0.6	2.7	2.1	0.74	24.5	54.7	30.2	3.41	65.3
2011.1	10/20-10/30	0.4	3.1	2.7	0.99	23.1	99.4	76.3	4.33	77.5
2011.2	11/13-11/26	1.6	30.0	28.4	3.35	75.9	280.9	205.0	5.32	92.5
2011.3	11/26-12/7	2.0	12.0	10.0	2.30	76.5	294.5	218.0	5.38	53.9
2011.4	12/7-12/25	2.1	45.0	42.9	3.76	90.3	753.2	662.9	6.50	177.0
2011.5	12/25-1/7	2.1	21.0	18.9	2.94	88.6	390.8	302.1	5.71	100.6
2011.6	1/11-2/2	1.5	200.0	198.5	5.29	74.2	1557.4	1483.2	7.30	134.6
2011.7	4/14-4/24	4.5	13.0	8.5	2.14	137.3	351.1	213.8	5.37	55.9
2012.1	11/10-11/21	0.6	4.7	4.1	1.41	27.8	138.8	110.9	4.71	104.9
2012.2	11/21-12/26	3.6	16.0	12.4	2.52	55.5	228.8	173.3	5.16	116.1
2012.3	12/27-1/16	0.3	150.0	149.7	5.01	35.1	906.1	871.0	6.77	131.6
2012.4	1/17-2/10	1.9	140.0	138.1	4.93	68.8	1226.1	1157.3	7.05	216.7
2012.5	2/17-3/3	1.8	8.3	6.5	1.87	106.8	373.8	267.0	5.59	82.1
2012.6	3/9-3/27	1.9	59.0	57.1	4.04	119.5	727.7	608.2	6.41	171.2
2012.7	3/29-4/10	4.8	76.0	71.2	4.27	161.4	909.0	747.6	6.62	102.1
2012.8	4/15-5/13	1.8	5.7	3.9	1.36	131.7	305.8	174.2	5.16	103.4

Event-storm identification, Tb$_{initial}$-turbidity at beginning of event, Tb$_{Max}$-Peak turbidity during event, deltaTb-change in turbidity from initial to peak, LogDTb-log of deltaT, Q$_{initial}$- discharge at beginning of event, Qmax-discharge Peak turbidity during event, DeltaQ-change in discharge from initial to peak, LogDQ-log of DeltaQ, Precipitation$_{Total}$-total precipitation during event

Linear models for Carter Bridge and Oregon City have R^2 values of "0.81" and "0.48", respectively. This illustrates that the log value of the change in discharge explains approximately 81% of the change in turbidity at Carter Bridge and approximately 48% of the change in turbidity at Oregon City.

Table 11.   Change in Turbidity Model Summary

Site	Estimate	Standard Error	t-value	p-value	Multiple R^2	Adjusted R^2	F-Statistic
Carter Bridge all Storms (n=41)	-2.74693	0.46679	-5.885	1.276 ^(-15)	0.82	0.81	170.4
Carter Bridge Wet Season Storms (n=33)	1.3669	0.1046	13.072	6.388e-14	0.85	0.85	170.9
Carter Bridge Dry Season Storms (n=8)	0.7470	0.1313	5.688	0.001274	0.84	0.82	32.36
Oregon City all Storms (n=41)	-2.194	0.8564	-2.562	2.761^(-7)	0.50	0.48	38.4
Oregon City Wet Season (n=33)	0.9528	0.1680	5.670	3.517e-06	0.52	0.50	32.15
Oregon City Dry Season (n=8)	Log ΔQ=1.249	0.24388	5.121	0.004579	0.88	0.84	19.06
	API3=0.029	0.01492	1.961				

4.6 Model Diagnostics for both sites

Diagnostic plots of linear regressions for Wet Season and Dry Season storms at Carter Bridge are shown in Figures 13 a-b and diagnostic plots of linear regressions for Wet Season and Dry Season storms at Oregon City are shown in Figures 14 a-b. Diagnostic plots of linear regressions for all storms at Carter Bridge and Oregon City are shown in Figures 15 a-b, respectively. These diagnostic plots are useful checks to determine if the multiple linear regression model is adequately representative of the data. There are four different plots for each model

The Residuals vs. Fitted plots for both sites in show a random pattern above and below the horizontal line at the midpoint in each case

The normal quantile-quantile plots for all models appear to demonstrate a normal distribution for all models. The quantile-quantile plots for Oregon City shows strong visual evidence of being normally distributed. Shapiro-Wilk (SW) tests for normality results on final model variables and residuals are listed in Appendix F.
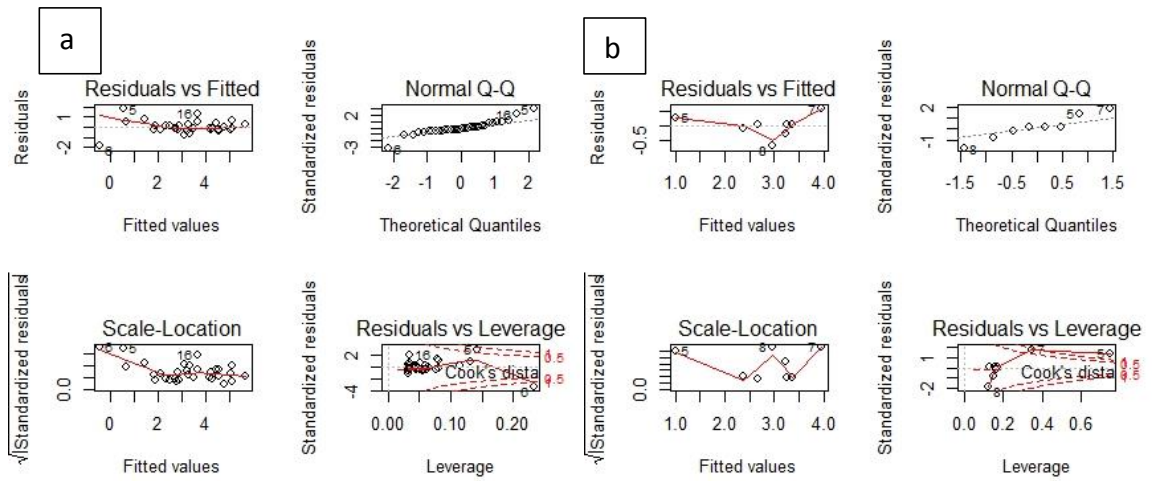
Figure 14. a-Diagnostic plots of Carter Bridge Wet Season model, b-Diagnostic plots of Carter Bridge Dry Season model
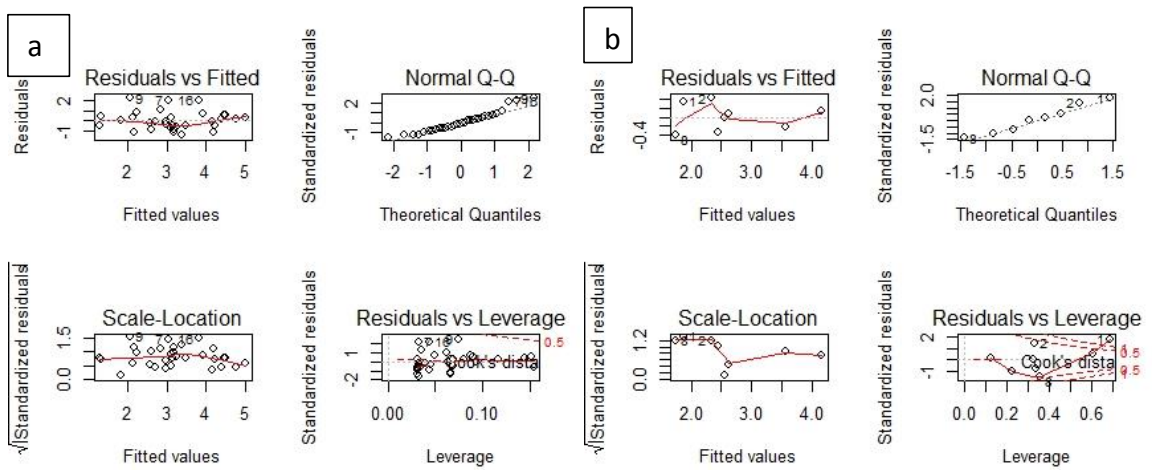
Figure 15. Diagnostic plots of Oregon City Wet Season model, b-Diagnostic plots of Oregon City Dry Season model
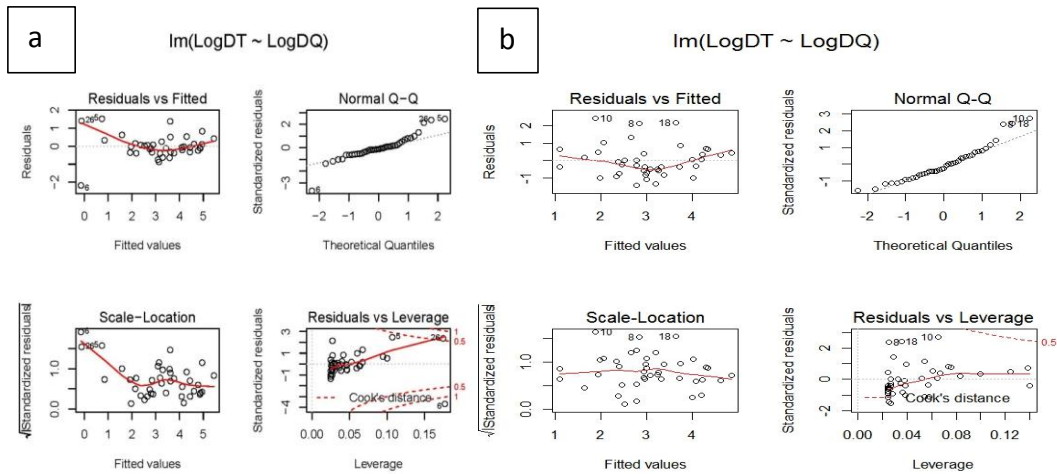
Figure 16. a-Diagnostic plots of Carter Bridge all Storms model, b-Diagnostic plots of Oregon City all Storms model

.

The Residuals versus Leverage is used to look for any influential data points that can have a visible effect on the model. Within this plot we are looking for outlying values in the upper right or lower right corners. These outlying values represent data points which can be influential against a regression line. We are also looking for cases outside of a dashed line. The Carter Bridge plot (figure 15a) has two data points outside, but were not deleted …in order to show distribution entire distribution of data points and the Oregon City plot 20d had no values outside of Cooks distance.

Results from covariance tests (Table 11) indicate that there is no strong evidence of serial autocorrelation in the residuals from either of the Carter Bridge and Oregon City models.

Table 12.   Results of Covariance Tests

Site	Breusch-Godfrey	BG p-value	Durbin Watson (DW)	DW p-value
Carter Bridge Final model	1.5407	0.4629	2.3326	0.8474
Oregon City Final Model	4.6004	0.1002	1.7762	0.2239

4.3 Turbidity Change During Storm Events

Box and whisker plots the minimum turbidity prior to a storm event, peak turbidity during the storm and change in turbidity from the minimum to the peak during the event are shown in Figure 16. In the majority of the comparisons the turbidity readings between the two sites appear to be somewhat similar when comparing the seasonal storm events.
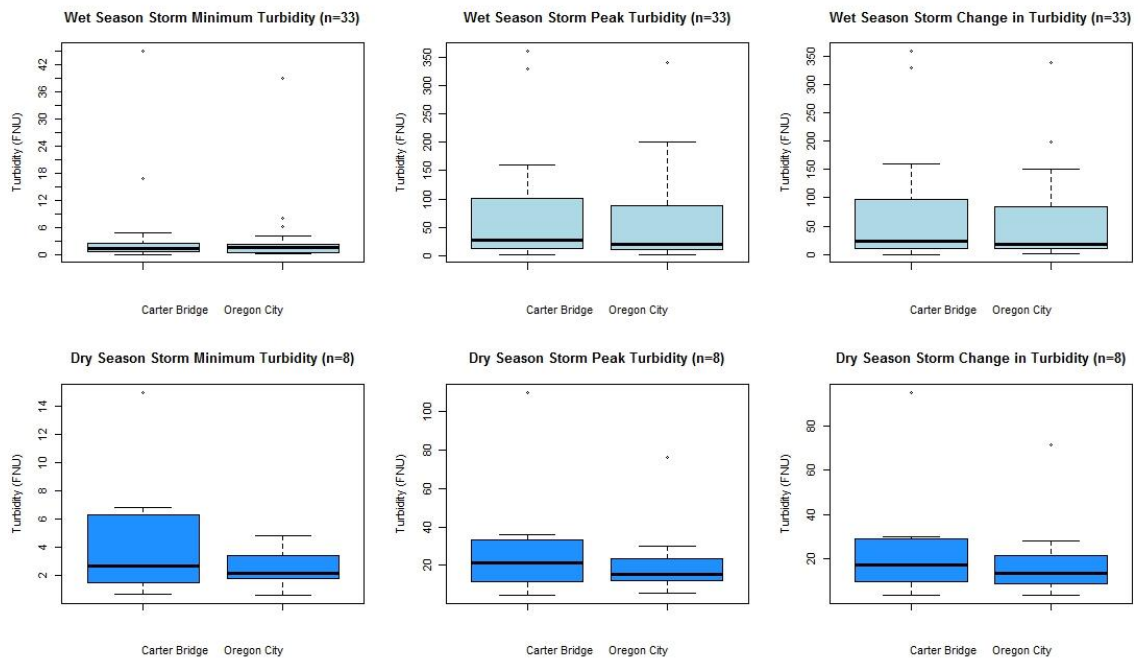
Figure 17. Boxplots of (a) minimum, (b) peak, and (c) change in turbidity during storm events

5. Discussion

Based on the method of calculating a hysteresis index (HI) at the midpoint of the hysteresis loop detailed by Lawler (2006) used in this analysis, overall, the majority of the storm events analyzed in this study exhibited a clockwise hysteresis pattern. This method was carefully selected for this study because of the importance of hysteresis as one of the many mechanisms that influences runoff during storm events. In comparison to the method of characterizing the properties of sediment discharge loops as detailed by other studies such as Seeger and others 2004 or Williams G. 1989, this method quantifies the magnitude and direction of the hysteretic affect in a single number and was used initially devised to be used with turbidity. Turbidity is a recognized surrogate for estimating suspended sediment concentrations and using an HI was better suited for this study than hysteretic loops.

Hysteresis is a rate-dependent non-linearity that is expressed through thresholds, switches and branches (Kane and Flynn, 2007). It is well established that soil moisture and precipitation are two of the primary influencing factors generating storm runoff. Subsequently soil moisture can be considered one of the critical switches that initiates storm runoff which further demonstrates the significance of taking hysteresis into account when investigating storm events.

5.1 Relation between land cover and hysteresis patterns

Many studies have investigated hysteresis effects in relation to turbidity and suspended sediment concentrations during storm events (Istok and Boesrma, 1986; House and Warwick, 1998; Sheeder and Ross, 2002; Chang and Carlson 2004; Eder et al., 2010; Gellis 2013; Dominic et al. 2015; Zhang et al. 2016). Seeger et al. (2004) investigated discharge and suspended sediment concentrations during storms in a small headwater catchment in the Spanish Pyrenees. They determined that clockwise hysteresis in mountain catchments can be explained by the rapid displacement of sediment from sources near the channel and the decrease of sediment before the decrease in discharge indicates that the sediment sources are limited and rapidly depleted. This is also a likely explanation for the majority clockwise hysteresis observed at Carter Bridge which has a mostly forested upstream landscape.

During counter-clockwise HI events sediment sources are widespread throughout the catchment and not exhausted rapidly (Seeger et al., 2004). Lawler et al. (2006) conducted their study in an urban river in the United Kingdom and found counterclockwise hysteresis to be the dominant pattern in their urban setting. They suggested that counter-clockwise hysteresis could be explained by sources of suspended solids being further away from monitoring stations and also to the complex drainage systems present in urban environments in comparison to forested and rural settings. In situations where delayed sub-surface runoff is important, stream water is expected to

be initially diluted in some solutes during storm runoff and be followed by higher

concentrations when the sub-surface components becomes and important contributor

(House and Warwick, 1997). The Oregon City monitoring station is located further

downstream and its water-quality is impacted by a complicated network of upstream

forested, agricultural and urban runoff sources. The higher number of counter-

clockwise hysteresis events at Oregon City in comparison to Carter Bridge may be

attributed to the combined agricultural and urbanization signature due to its

downstream location and tributaries that drain urban and suburban areas that have

more complex landscapes in comparison to the forested upstream location of the Carter

Bridge .

Increased turbidity during storm events is largely influenced by eroded sediment

particles entering the stream from the near stream zone and upstream tributaries in the

basin. Soil erosion and subsequent sediment transport into a waterway involves

detachment, entrainment and eventual transport of particles via the stream network.

In comparison to Carter Bridge, Oregon City has additional inputs from tributaries in the

lower basin with the upstream influences of agricultural and urban development. This

difference in tributary inputs must be taken into account when comparing turbidity

measured during storms between the two stations. Agricultural practices affect the

quantity of runoff through alteration of evaporation, the timing of runoff through

changes in land drainage and water quality through erosion. Hydrologic consequences

include siltation of water courses and reservoirs and an increase in flood peaks and a

reduction in river low flows as vegetation and soil are removed from hill lands (Pimintel, 1976). As land urbanizes, it is covered by impervious surfaces and paved roads, parking lots, and roofs which prevent rainfall or snowmelt from infiltrating into the ground. Surface runoff in urban areas has a higher velocity than in nonurban areas because imperious surfaces are smoother than meadow, range land, forest or farm fields (Urbonas and Roesner, 1993). Once runoff starts, the quantity and size of material transported increases with the velocity of water runoff (Barfield and Warner, 1981). Particles transported in urban areas to rivers and streams contribute to increased turbidity during storm events. The larger tributaries in the northern part of the lower Clackamas Basin include Deep, Rock, and Sieben Creeks (Figure 1) contribute to runoff into the Clackamas River and runoff from this portion of the basin are not measured upstream at Carter Bridge.

Rock and Sieben Creeks drainage area (Figure 1) is roughly about 25 km^2. In contrast to areas upstream of Carter Bridge (>88% forested) is classified as 33% forested (USGS, StreamStats) and the rest of this sub-basin is classified as 28% agriculture (cultivated crops), and the remaining portion of the land cover is classified as developed from low to high intensity. Storm water runoff from impervious surface area (12.4%) originating from the urbanized lower basin would be likely to account for some of the differences in turbidity observed during storm events in comparison to upstream at Carter Bridge.

67

5.2 Effects of discharge on changes in turbidity

Multiple linear regression (MLR) is an effective tool that can be used to explain the variation in a dependent variable (y), by using one or more explanatory variables. Antecedent precipitation index (API) of 3, 5, 7, 14 and 30 days, total precipitation (P) and change in discharge were the explanatory variables used to determine which one (or combination) of these variables best explained the change in turbidity during storms. It is well documented in literature that soil moisture conditions and precipitation are primary determinants in runoff during storm events (Nikas, 2007; Bousfield, 2008; Shakir, 2010; Tramblay, 2012). Results from MLR indicated that the model using change in discharge [ΔQ=Natural Log (Ln) of change in discharge] during a storm-event best explains the magnitude of turbidity during storms. The model developed for Carter Bridge and Oregon City using the log value of the change in discharge explained 81% of the change in turbidity at Carter Bridge and 48% of the change in turbidity for Oregon City during the 41-storm events selected for this study.

Results of MLR model surprisingly did not show any of the API indices to be one of the variables that contributed to the "best fit" results. In a few studies where API was the explanatory variable for runoff amounts (Fedor and Bescht, 1989)-API were directly related to storm runoff], (Nikas et al., 2007), found a correlation between API and runoff

volume, (Ali et Al., 2010)—All found correlations with rainfall runoff amounts. ---This correlation did not translate to API in looking at changes in turbidity in this investigation. Onderka (2012) suggests that "complex systems (e.g. catchments) are most often hindered by interfering responses caused by several sub-processes that interact in time and space. It is very possible that the log "change in discharge" variable incorporates the processes of API and total precipitation and when the variables are regressed in the equations the "change in Q" variable overshadows the individual effect of API's and total precipitation. There is a correlation between the explanatory variables selected and it is a possible explanation as to why neither of the individual API's or precipitation-total did not individually have representative coefficients in the final model equations.

5.3 Implications for water management and potential model improvement

The Oregon City site, located in the lower portion of the Clackamas Basin, is more impacted by upstream agriculture and urban development, and based on calculated HI values, it had more than three-times more likely to have counter clockwise hysteresis, with higher turbidity on the falling limb of the storm hydrograph than the upstream primarily forested Carter Bridge site. This information can be very important for water management agencies and drinking water providers in the basin. Knowing that a system is likely to have increased particulate matter (higher turbidity) on the recession limb of a hydrograph could inform management strategies in three ways that

could lessen exposure to pollutants that are higher during storm runoff events, minimize costs for water treatment and provide real-time warnings of conditions that might prove detrimental to source-water quality and therefore the quality of finished water for drinking water providers that use water from the Clackamas River. High turbidity conditions can be detrimental to water treatment, and such conditions may be avoided with sufficient flexibility in planning, system storage, and operations.

The Clackamas Basin encompasses an area of 2,440 km^2 of forested and rural land in the upper basin; with some agricultural and urban land in the lower basin. Studies have shown that the lack of spatially and temporally distributed rainfall data can have a serious impact on watershed runoff generation (Sun and others, 2002). Several factors must be considered attempting to understand the hydrological control that affect storm events in the basin. Precipitation is not uniformly distributed over the entire basin during storm events, therefore including spatially-varying precipitation amounts in different locations within the basin should improve our model results.

6. Summary and Conclusions

6.1 Summary

This research answers the three questions stated in the introduction:

- In respect to the first research question:

"Are there any differences in turbidity measured during high-flow storm events between the Carter Bridge (upstream) and Oregon City (downstream) water-quality monitoring stations on the Clackamas River?"

Paired -t-tests results showed, of the 41 storm-events compared, turbidity values during storms between the two sites were statistically different. This is strong evidence that the two stations respond differently during storm events.

- In respect to the second research question

"What are the dominant hysteresis regimes in both stations by season?"

HI results showed that clockwise hysteresis (C) was the most common pattern of HI at both sites, and Oregon City was "3-times" more likely to exhibit counter-clockwise (CC) hysteresis in comparison to Carter Bridge. The likely reason for this is that (C) hysteresis during storm events is due to turbidity peaks proceeding peaks in discharge and likely caused by depletion of sediments deposited in channels or near stream areas. The opposite CC is likely due to more complex particles introduced from complex urban

environments and agricultural environments and by later arriving sediments from sub-basins located in the lower portion of the Clackamas Basin.

- In respect to the third research question:

"Of the following parameters: antecedent precipitation index (API), total precipitation and discharge and which one, or combination of these parameters are the major controls that determine the magnitude of turbidity measured during storm events turbidity during storm events?" MLR model showed that the "Log change in discharge" best explained the "change in turbidity". A number of the model equations generated by the MLR did have coefficients for API values, but they were negative coefficients and not used in the final model. The log value of the change in discharge explains approximately 81% of the change in turbidity at Carter Bridge and 48% of the change in turbidity at Oregon City.

Conclusions

Storm events in the Clackamas Basin for purposes of the study particulate matter resulting increased turbidity (which can be attributed to sediment in the water column) are limited to sediment and other particles near the stream channel. Similar conclusions suggested that observed hysteresis might be due to early episode flushing of soluble material (Walling and Foster, 1975), McKee et. al. (2000) attributed nutrient

concentrations during storm events to similar hysteresis patterns by the flushing of material on the rising limb of a hydrograph during storms.

6.2 Suggested Additional Research

 Further investigation into the research questions would likely focus on having concurrent suspended sediment concentration and particle size analysis. With this additional information it would be possible to establish a correlation and measurable relationship between the turbidity and suspended sediment concentration. Additional sample collection and turbidity measurement in the lower basin would also give information about the differences in particles mobilized during events between the forested upstream flow regimes and the more mixed land-use flow regimes.

It would also be beneficial to obtain discharge measurements at Carter Bridge instead of using discharge measurements from the upstream Three Lynx station as a surrogate for discharge at Carter Bridge.

References

Ali S., Ghosh N. and Singh R., 2010, Rainfall–runoff simulation using a normalized antecedent precipitation index, Hydrological Sciences Journal, 55:2, 266-274

American Public Health Association, American Water Works Association, and Water Environment Federation. 1998. Standard methods for the examination of water and wastewaters (20th Ed.). American Public Health Association, Washington, D.C., pp. 2-8 to 2-11.

Anderson, C.W., and Rounds, S.A., 2003, Phosphorus and *E. coli* and their relation to selected constituents during storm runoff conditions in Fanno Creek, Oregon, 1998-99: U.S. geological Survey Water-Resources Investigations Report 02-4232, 34 p.

Anderson C.W., 2006, Turbidity (ver. 2.1): U.S. Geological Survey Techniques of Water-Resources Investigations, book 9, chap. A6., sec. 6.7, September, 2005 accessed [March 30, 2014], from http://pubs.water.usgs.gov/twri9A6/.

ASTM International, 2003a, D1889–00 Standard test method for turbidity of water, *in* ASTM International, Annual Book of ASTM Standards, Water and Environmental Technology, 2003, v. 11.01, West Conshohocken, Pennsylvania, 6 p.

Barfield B., Warner R., 1981, Applied Hydrology and sedimentation for disturbed areas,

Berrie, A. D., 1993, The rivers handbook volume 1: Hydrological and ecological principles, edited by P. Calow and G. E. Petts, Blackwell Scientific Publications, Oxford. 526 pp.

Bragg H., Sobieszczyk, S., Uhrich, M., and Piatt D., 2007, Suspended-sediment loads and yields in the North Santiam river basin, Oregon, water years 1999-2004: U.S. Geological Survey Scientific Investigations Report 2007-5187, 26 p.

Calder I., 1993, Hydrologic Effects of Land Use Change section 13.1, published in Handbook of hydrology David Maidment Editor McGraw-Hill Inc.

Cannon A., Whitfield P., 2001 Modeling Transient pH Depressions in Coastal Streams of British Columbia using Neural Networks Journal of the American Water Resources Association Volume 37, 1, 73-89

Carpenter K., 2003, Water Quality and Algal Conditions in the Clackamas River Basin, Oregon and their Relations to Land and Water Management, U.S. Geological Survey WRIR 02-4189

Chang H., 2007, Comparative stream flow characteristics in urbanizing basins in the Portland Metropolitan Area, Oregon, USA, Hydrological Processes 21, 211-222

Chanson H., Takeuchi M., Trevethan M., 2008 Using turbidity and acoustic backscatter intensity as surrogate measures of suspended sediment concentration in a small subtropical estuary. Journal of Environmental Management 88, 1406-1416

Chen H., Chang, H., 2014 Response of Discharge, TSS, and E.coli to Rainfall Events in Urban, Suburban, and Rural Watersheds. Environmental Science: Processes and Impacts 16 (10): 2313 – 2324

Clackamas River Water Providers Website, 2017, http://www.clackamasproviders.org/crwp-members/ accessed 3/1/2017

Davie T., 2008, Fundamentals of Hydrology, 2nd ed., pg. 132, by Routledge Taylor and Francis Group

Davies-Colley, R.J., and Smith, D.G., 2001, Turbidity, suspended sediment, and water clarity—A review: Journal of the American Water Resources Association, v. 37, no. 5, p. 1085–1101.

Driver, N. E., Troutman B.M., 1988, Regression Models for Estimating Urban Storm-Runoff Quality and Quantity in the United States Journal of Hydrology, 109 (1989) 221-236 221 Elsevier Science Publishers B.V., Amsterdam -- Printed in The Netherlands

Eckhardt K., 2008, A comparison of baseflow indices, which were calculated with seven different baseflow separation methods, Journal of Hydrology 352, 168-173

Esralew, R.A., Andrews, W.J., and Smith, S.J., 2011, Evaluation and trends of land cover, stream flow, and water quality in the North Canadian River Basin near Oklahoma City, Oklahoma, 1968–2009: U.S. Geological Survey Scientific Investigations Report 2011–5117, 97 p. (Revised October 2011)

Evans, C. and Davies, T.D., 1998, Causes of concentration/discharge hysteresis and its potential as a tool for analysis of episode hydrochemistry, Journal of the American Water Resources Association 38 (4):1027-1040.Fausch, Kurt D.; Torgersen, Christian E.;

Fedora M.A. and Beschta R.L., 1989, Storm Runoff Simulation using an Antecedent Precipitation Index (API) Model, Journal of Hydrology, 112, 121-133 Elsevier Science Publishers B.V., Amsterdam- Printed in The Netherlands

Fletcher T.D. and Deletic, 2007 Statistical evaluation and optimization of storm water quality monitoring programs Water Science & Technology Vol 56 No 12 pp 1–9 *Q*

Foster I., 1978, a Multivariate Model of Storm-Period Solute Behaviour. Journal of Hydrology, 39, 339-353 Elsevier Science Publishers B.V., Amsterdam- Printed in the Netherlands

Gering A.J., 1985, Soil Survey of Clackamas County Oregon, United States Department of Agriculture, Soil Conservation Service in cooperation with United States Department of Interior, Bureau of Land Management and Oregon Agricultural Experiment Station

Gippel, C., 1989, Use of turbidimeters in suspended sediment research: Hydrobiologia, v. 176, no 17, p. 74-76

Gippel, C. 1995, Potential of turbidity monitoring for measuring the transport of suspended solids in streams, Hydrol. Processes, 9, 83-97

Graves D., and Chang H., 2007, Clim Res. Vol. 33: 143–157

Gray J., and Glysson D., 2003, Proceedings of the federal interagency workshop on turbidity and other sediment surrogates, April 30-May 2, 2002, Reno, Nevada: U.S. Geological Survey Circular 1250, 56 p.

Helsel D.R., and Hirsch Statistical Methods in Water Resources, 2002, Techniques of Water-Resources Investigations of the United States Geological Survey Book 4, Hydrologic Analysis and Interpretation Chapter A3, Publication available at: http://water.usgs.gov/pubs/twri/twri4a3/
Horowitz, A., 1991 A primer on sediment-trace element chemistry 2nd rev.ed. by Lewis Publishers, Inc.

Homer, C.H., Fry, J.A., and Barnes C.A., 2012, The National Land Cover Database, U.S. Geological Survey Fact Sheet 2012-3020, 4 p. (https://www.mrlc.gov/nlcd11_data.php)

House, William A., and Warwick Melanie S., 1998, Hysteresis of the solute concentration/discharge relationship in rivers during storms. Water Research, 32(8): 2279-2290

International Organization for Standardization, Reference number ISO 7027:1999(E) 1999, International Standard ISO 7027 was prepared by Technical Committee ISO/TC 147, Water quality, Subcommittee SC 2, Physical, chemical, biochemical methods.

Istok J., Boersma L., 1986 Journal of Hydrology, 88, 329-342 Elsevier Science Publishers B.V., Amsterdam -- Printed in the Netherlands

Langan S., and Hirst D., 2004, An analysis of the long-term variation in stream water quality for three upland catchments at Loch Dee (Galloway, S.W. Scotland) under contrasting land management, Hydrology and Earth Systems Sciences, 8 (3), 422-435

Larson, S., Capel P., Majewski M., 1997 Pesticides in surface waters: distribution, trends, and governing factors, Volume Three of the Series Pesticides in the Hydrologic System—Ann Arbor Press, Inc.

Lawler D., Petts G., Foster I., Harper S., 2006, Turbidity dynamics during storm events in an urban headwater river system: The Upper Tame, West Midlands, UK Science of the Total Environment 360, 109-126

McCutcheon S., Martin J., Barnwell T., 1993, Water Quality section 11.1.5, published in Handbook of hydrology David Maidment Editor McGraw-Hill Inc.

McKee L., Bradley E., Shahadat H., 2000, Intra- and interannual export of nitrogen and phosphorus in the subtropical Richmond River catchment, Australia, Hydrol. Process 14, 1787-1809,

Meene. J., Williams C. and Vose R., 2013. United States Historical Climatology Network Daily Temperature, Precipitation, and Snow Data. Carbon Dioxide Information Analysis Center, Oak Ridge National Laboratory, Oak Ridge, Tennessee. Available on-line: (http://cdiac.ornl.gov/epubs/ndp/ushcn/ushcn.html) from the Carbon Dioxide Information Analysis Center, Oak Ridge National Laboratory, Oak Ridge, Tennessee.

Metro, 1997, Clackamas River Watershed Atlas: Portland, Oregon, Metro Regional Services, 41 p.

Meybeck M. and Moatar F., 2012, Daily variability of river concentrations and fluxes: indicators based on segmentation of the rating curve, Hydrological Processes 26, 1188-1207

Nikas K., Antonakos A., Lambrakis N., and Kallergis G., 2007, THE USE OF ANTECEDENT PRECIPITATION INDEX AND "DELAY FACTOR" TO ESTIMATE RUNOFF FROM RAINFALL; A CASE STUDY FROM EIGHT DRAINAGE BASINS -ACHAIA, PELOPONESSOS, GREECE., Bulletin of the Geological Society of Greece vol. XXXX, 2007 Proceedings of the 11 th International Congress, Athens, May

Onderka M., Andreas K., Wrede S., Martínez-Carreras N., Hoffmann L., 2012, Dynamics of storm-driven suspended sediments in a headwater catchment described by multivariable modeling- J Soils Sediments 12:620–635--Reference for antecedent conditions and table showing storm events

Pidwirny, M., 2006, Climate Classification and Climatic Regions of the World". *Fundamentals of Physical Geography, 2nd Edition*

Prestigiacomo A., Steven E., O'Donnell D., Hassett J., Michalenko E., Lee Z., and Weidemann A., 2007, Turbidity and suspended solids levels and loads in a sediment enriched stream: implications for impacted lotic and lentic ecosystems, Lake and Reservoir Management, 23:3, 231-244

Rantz, S, 1982, Measurement and computation of stream flow (Geological Survey Water-Supply Paper 2175) Includes bibliographies. Contents: v. 1. Measurement of stage and discharge.- v. 2. Computation of discharge. 1. Stream measurements.

Rasmussen, T., Lee, C., and Ziegler, A., 2008, Estimation of constituent concentrations, loads, and yields in streams of Johnson County, northeast Kansas, using continuous water-quality monitoring and regression models, October 2002 through December 2006: U.S. Geological Survey Scientific Investigations Report 2008–5014, 103 p.

Rutledge A.T., 1993 Computer programs for describing the recession of ground-water discharge and for estimating mean ground-water recharge and discharge from streamflow records U.S. Geological Survey Water Resource Investigations Report 93-4121 45 p.

Settle S., Ashantha G., and Godwin A., 2007, Determination of Surrogate Indicators for Phosphorus and Solids in Urban Storm water: Application of Multivariate Data Analysis Techniques Water Air Soil Pollution 182:149–161

Sadar M., 1999, Turbidimeter Instrument Comparison: Low-level Sample Measurements. Hach Company, all rights reserved Printed in U.S.A. D90.5

Seeger M., Erreab M., Beguerı´ab S., Arna´ezc J., Martı´b C., Garcı´a-Ruiz J., 2004 Catchment soil moisture and rainfall characteristics as determinant factors for discharge/suspended sediment hysteretic loops in a small headwater catchment in the Spanish Pyrenees., Journal of Hydrology 288, 299–311 http://www.elsevier.com/locate/jhydrol

Shedder, S., Ross J., and Carlson T., 2002, Dual urban and rural hydrograph signals in three small watersheds. Journal of the American Water Resources Association 38 (4):1027-1040

Sun H., Cornish P.S., Daniel T.M., 2002, Spatial Variability in Hydrologic Modeling Using Rainfall-Runoff Model and Digital Elevation Model, , J. Hydrol. Eng. 7:404-412

Taylor B., 1999, Salmon and Steelhead Runs and Related Events of the Clackamas River Basin-A Historical Perspective, Prepared for Portland General Electric (PGE). for copies contact: PGE Hydro Licensing Department 121 SW Salmon St. Portland, OR 97204

Tramblay Y., Bouaicha R., Brocca L., Dorigo W., Camici S., Servat E., 2012, Estimation of antecedent wetness conditions for flood modelling in northern Morocco, Hydrology and Earth System Sciences, 16, 4375-4386

Uhrich, M., Bragg H., 2003, Monitoring in stream turbidity to estimate continuous suspended-sediment loads and yields and clay-water volumes in the Upper Santiam River Basin, Oregon, 1998-2000: U.S. Geological Survey Water-Resources Investigations Report 03-4098, 43 p.

Uhrich, M., Kolasinac J., Booth P., Fountain L., Spicer K., and Mosbrucker R.,2014, Correlations of Turbidity to Suspended-Sediment Concentration in the Toutle River Basin, near Mount St. Helens, Washington, 2010–11, 2014, Geological Survey Open-File Report 2014-1204, 30 p.,

Urbonas B., Roesner L., 1993, Hydrologic Design for Urban Drainage and Flood Control, published in Handbook of hydrology David Maidment Editor McGraw-Hill Inc.

U.S. Geological Survey, 2016, The StreamStats program, online at http://streamstats.usgs.gov, accessed on (4/13/2017).

Van Dijk A., 2010, Climate and terrain factors explaining stream flow response and recession in Australian catchments. Hydrol. Earth Syst. Sci., 14, 159–169

Verzani J., 2004, Using R for introductory statistics, CRC Press Taylor and Francis Group, LLC

Vicenzo, A., Molino, B., Viparelli R., Caramiscia P., 2011A methodological approach for estimating turbidity in a river, International Journal of Sediment Research 26, 112-119

Wagner, R., Boulger, R., Jr., Oblinger, C., Smith, B., 2006, Guidelines and standard procedures for continuous water-quality monitors—Station operation, record computation, and data reporting: U.S. Geological Survey Techniques and Methods, Book 1, Chapter D3.

Walling, D., Foster I., 1975, Variations in natural chemical concentration of river water during flood flows, and the lag effect: Some further comments, J. Hydrol.,26, 237-244,

Walling, D., Webb B., 1998, the reliability of rating curve estimates of suspended sediment yield: some further comments, in Sediment Budgets, IAHS Publ. 174, pp. 337-350

Ward A., Trimble S., 2004, Environmental Hydrology Second Edition pg. 59, CRC Press LLC, Lewis Publishers

Wass P., Marks S., Finch J., Leeks G., Ingram J., (1997) Monitoring and preliminary interpretation of in-river turbidity and remote sensed imagery for suspended sediment transport studies in the Humber catchment. The Science of the Total Environment 194/195 263-283

Williams G., 1989, J Suspended Sediment Concentration vs. Discharge during Single Hydrologic Events in Rivers, Journal of Hydrology, 111, 89-106 89. Elsevier Science Publishers B.V.,Amsterdam printed in Netherlands

Yellow Springs Incorporated (YSI) Incorporated Environmental Monitoring Systems Manual pg. 5-18, Item #069300 Revision E April, 2009

Appendix A-Statistical Summary of Turbidity and Discharge Data for Clackamas at Carter Bridge and Oregon City Sites

Turbidity Data Water Years 2006-2012 Discharge Data Water Years 2006-2012

Statistic	Carter Bridge (FNU)	Oregon City (FNU)	Statistic	Carter Bridge (Three Lynx) (CMS)	Oregon City (CMS)
Mean	5.1	4.5	Mean	70.6	106.3
Standard Deviation	18.5	14.2	Standard Deviation	62.2	111.0
IQR	2.7	2.7	IQR	59.1	101.0
Minimum	0	0	Minimum	18.3	21.1
25%	0.7	0.7	25%	29.0	32.3
Median	1.5	1.4	Median	55.4	81.3
75%	3.4	3.4	75%	88.1	133.2
Maximum	340	340	Maximum	674.2	1413.0
n	2509	2535	n	2557	2454
Missing Values	48	22	Missing Values	0	103

FNU=formazin nephelometric units, CMS=cubic meters per second, IQR=interquartile range

Appendix B-Annual Precipitation Data Summary Measured at Clackamas at Three Lynx for Water Years 2006-2012

Month	Water Year 2006 (mm)	Water Year 2007 (mm)	Water Year 2008 (mm)	Water Year 2009 (mm)	Water Year 2010 (mm)	Water Year 2011 (mm)	Water Year 2012 (mm)	Monthly Average (mm)	Standard Deviation
October	142.2	639.1	188.0	228.3	269.2	292.1	233.4	284.6	164.7
November	303.3	299.5	382.8	241	186.7	357.1	211.3	283.1	73.4
December	356.4	166.9	280.2	197.6	213.1	207.3	424.9	263.8	95.2
January	475	270	162.1	181.9	128.5	199.4	210.1	232.4	115.6
February	139.2	108.5	190	229.1	241.3	243.8	393.2	220.7	92.2
March	144.3	104.4	151.6	165.9	177.5	257.3	176.8	168.3	46.6
April	130.3	49.8	109	159.3	16.3	131.6	101.6	99.7	36.3
May	68.3	48.5	66.3	51.3	164.6	50.5	145	84.9	48.7
June	1.0	8.4	2.3	8.9	13.2	29.7	10.4	10.6	9.5
July	6.1	27.7	62.5	6.9	0.0	4.6	0.3	15.4	22.8
August	35.3	65.5	28.7	45.5	106.4	9.1	1.8	41.8	35.7
September	100.6	172	90.2	195.1	153.4	114.3	232.2	151.1	52.5

m=millimeters

Appendix C Annual Precipitation Data Summary at Three Lynx and Oregon City for years 2006-2012

Water Year 2006		
Statistic	**Three Lynx**	**Oregon City**
Mean	5.2	3.2
Standard Deviation	10.3	7.5
IQR	5.1	1.8
0%	0.0	0.0
25%	0.0	0.0
50%	0.0	0.0
75%	5.1	1.8
100%	71.1	50.8
n	365	320
Missing	0	45

Water Year 2007		
Statistic	**Three**	**Oregon City**
Mean	5.4	1.6
Standard deviation	11.2	4.9
IQR	5.3	0.8
0%	0.0	0.0
25%	0.0	0.0
50%	0.0	0.0
75%	5.3	0.8
100%	102.4	50.8
n	365	341
Missing	0	24

Annual Precipitation Data Summary at Three Lynx and Oregon City for years 2006-2012 (cont.)

Water Year 2008		
Statistic	Three Lynx	Oregon City
Mean	4.7	3.2
Standard Deviation	8.2	7.7
IQR	6.8	1.8
0%	0.0	0.0
25%	0.0	0.0
50%	0.1	0.0
75%	6.8	1.8
100%	47.0	50.8
n	270	366
Missing	96	0

Water Year 2009		
Statistic	Three Lynx	Oregon City
Mean	4.7	2.2
Standard Deviation	9.4	6.2
IQR	5.1	1.3
0%	0.0	0.0
25%	0.0	0.0
50%	0.0	0.0
75%	5.1	1.3
100%	64.8	63.5
n	365	327
Missing	0	38

Annual Precipitation Data Summary at Three Lynx and Oregon City for years 2006-2012

Water Year 2010		
Statistic	**Three Lynx**	**Oregon City**
Mean	4.9	3.1
Standard Deviation	8.8	6.5
IQR	6.4	2.5
0%	0.0	0.0
25%	0.0	0.0
50%	0.3	0.0
75%	6.4	2.5
100%	49.5	49.5
n	365	362
Missing	0	3

Water Year 2011		
Statistic	**Three Lynx**	**Oregon City**
Mean	5.2	3.9
Standard Deviation	9.4	8.2
IQR	6.9	4.1
0%	0.0	0.0
25%	0.0	0.0
50%	0.8	0.0
75%	6.9	4.1
100%	75.2	50.8
n	365	365
Missing	0	0

Annual Precipitation Data Summary at Three Lynx and Oregon City for years 2006-2012

Water Year 2012		
Statistic	**Three Lynx**	**Oregon City**
Mean	5.8	3.4
Standard Deviation	12.3	8.1
IQR	6.5	2.5
0%	0.0	0.0
25%	0.0	0.0
50%	0.0	0.0
75%	6.5	2.5
100%	120.7	58.2
n	366.0	366.0
Missing	0	0

Appendix D-Summary and Statistical Information of Wet Season and Dry Season Turbidity and Discharge

Wet Season (October-March)   **Wet Season (October-March)**

Turbidity Data 2006-2012   **Discharge Data 2006-2012**

Statistic	Carter Bridge (FNU)	Oregon City (FNU)	Statistic	Carter Bridge (Three Lynx) (CMS)	Oregon City (CMS)
Mean	8.2	7.3	Mean	82.5	131.4
Standard Deviation	22.6	19.5	Standard Deviation	74.4	134.5
IQR	4.0	5	IQR	54.4	97.1
Minimum	0	0	Minimum	21.8	22.0
25%	1.1	1	25%	39.6	53.5
Median	2.2	2.4	Median	62.6	92.6
75%	5.1	6	75%	94.0	150.7
Maximum	340	340	Maximum	674.2	1413.0
n	1254	1271	n	1276	1273
Missing Values	22	5	Missing Values	0	3

Dry Season (April-September)

Turbidity Data 2006-2012

Dry Season (April-September)

Discharge Data 2006-2012

Statistic	Carter Bridge	Oregon City	Statistic	Carter Bridge (Three Lynx)	Oregon City
Mean	22.1	1.6	Mean	58.7	79.3
Standard Deviation	22.9	2.1	Standard Deviation	45.4.0	68.6
IQR	26.0	1.1	IQR	58.0	86.9
Minimum	1.0	0	Minimum	18.3	21.1
25%	7.0	0.6	25%	26.8	27.2
Median	11.0	0.9	Median	36.5	47.9
75%	33.0	1.7	75%	84.9	114.1
Maximum	96.0	26	Maximum	311.0	472.9
n	1281	1264	n	1281	1181
Missing Values	0	17	Missing Values		100

Appendix E- Hysteresis Indices for Carter Bridge

Hysteresis Indices and Associated Data from Clackamas at Carter Bridge									
Event ID	WY 2006 Dates	Qmin (M^3/sec)	Qmax (M^3/sec)	Qmid (M3/sec)	Qrising (TU$_{RL}$)	Qfalling (TU$_{FL}$)	Season	HI	HD
2006.1	11/10-11/24	41.1	85.8	63.4	14	1.6	wet	7.75	C
2006.2	12/18-12/26	25.3	354.0	189.6	45	47	wet	-0.04	CC
2006.3	12/29-1/6	184.6	560.7	372.6	110	92	wet	0.20	C
2006.6	1/28-2/11	74.2	219.7	147.0	22	8.4	wet	1.62	C
2006.7	2/27-3/5	45.9	62.6	54.2	3	0.3	wet	9.00	C
2006.8	3/7-3/12	49.6	57.8	53.7	1.2	3.9	wet	-2.25	CC
2006.9	4/2 -4/30	52.1	103.6	77.9	17	2.2	dry	6.73	C
Event ID	WY 2007 Dates	Qmin (M^3/sec)	Qmax (M^3/sec)	Qmid (M3/sec)	Qrising (TU$_{RL}$)	Qfalling (TU$_{FL}$)	Season	HI	HD
2007.1	10/31 -11/12	20.5	515.4	267.9	170	100	wet	0.70	C
2007.2	12/8-12/22	63.7	356.8	210.3	34	32	wet	0.06	C
2007.3	12/22-1/7	84.1	253.2	168.6	29	12	wet	1.42	C
2007.6	3/24-4/1	69.7	122.9	96.3	11	2.7	wet	3.07	C
Event ID	WY 2008 Dates	Qmin (M^3/sec)	Qmax (M^3/sec)	Qmid (M3/sec)	Qrising (TU$_{RL}$)	Qfalling (TU$_{FL}$)	Season	HI	HD
2008.1	10/15-10/26	19.2	113.3	66.2	11	2.8	wet	2.93	C
2008.2	11/15-11/26	98.5	186.0	142.3	9.6	21	wet	-1.19	CC
2008.3	12/1-12/16	35.1	501.2	268.2	63	38	wet	0.66	C
2008.5	5/14-5/28	91.7	283.2	187.5	22	12	dry	0.83	C

Event ID	WY 2009 Dates	Qmin (M^3/sec)	Qmax (M^3/sec)	Qmid (M3/sec)	Qrising (TU$_{RL}$)	Qfalling (TU$_{FL}$)	Season	HI	HD
2009.1	10/27-11/5	22.6	40.8	31.7	3	0.9	wet	2.33	C
2009.2	11/5-11/18	36.8	288.8	162.8	59	24	wet	1.46	C
2009.3	12/23-1/20	26.4	194.3	110.3	14	6.7	wet	1.09	C
2009.4	2/21-3/17	31.7	122.3	77.0	14	3.5	wet	3.00	C
2009.5	5/4-5/31	88.1	258.0	173.0	22	8.8	dry	1.50	C
Event ID	WY 2010 Dates	Qmin (M^3/sec)	Qmax (M^3/sec)	Qmid (M3/sec)	Qrising (TU$_{RL}$)	Qfalling (TU$_{FL}$)	Season	HI	HD
2010.1	11/5 - 11/16	26.1	69.4	47.7	4.6	1.5	wet	2.07	C
2010.2	12/9 - 12/30	26.2	145.3	85.7	10	4.1	wet	1.44	C
2010.3	1/4 - 1/15	82.1	192.8	137.5	14	6.6	wet	1.12	C
2010.4	3/28-4/5	55.5	303.0	179.2	68	20	wet	2.40	C
2010.5	6/1 - 6/22	52.1	216.6	134.4	8.6	5.7	dry	0.51	C
2010.6	9/14-10/2	21.6	30.0	25.8	1.8	1.4	dry	0.29	C
Event ID	WY 2011 Dates	Qmin (M^3/sec)	Qmax (M^3/sec)	Qmid (M3/sec)	Qrising (TU$_{RL}$)	Qfalling (TU$_{FL}$)	Season	HI	HD
2011.1	10/20-10/30	22.3	55.2	38.8	3.8	2.5	wet	0.52	C
2011.2	11/13-11/26	38.2	122.3	80.3	8.6	5.2	wet	0.65	C
2011.3	11/26-12/7	49.0	111.0	80.0	18	3.2	wet	4.63	C
2011.4	12/7-12/25	40.2	305.8	173.0	36	23	wet	0.57	C
2011.5	12/25-1/7	50.7	121.2	85.9	18	6	wet	2.00	C
2011.6	1/11-2/2	39.9	775.9	407.9	130	120	wet	0.08	C

Event ID	WY 2012 Dates	Qmin (M^3/sec)	Qmax (M^3/sec)	Qmid (M3/sec)	Qrising (TU$_{RL}$)	Qfalling (TU$_{FL}$)	Season	HI	HD
2011.7	4/14-4/24	74.2	151.8	113.0	23	12	dry	0.92	C
2012.1	11/10-11/21	21.2	85.5	53.4	NA	NA	wet	NA	C
2012.2	11/21-12/26	30.9	156.6	93.7	41	7.9	wet	4.19	C
2012.3	12/27-1/16	22.7	481.4	252.0	210	60	wet	2.50	C
2012.4	1/17-2/10	24.9	518.2	271.6	130	38	wet	2.42	C
2012.5	2/17-3/3	56.9	187.5	122.2	14	5.5	wet	1.55	C
2012.6	3/9-3/27	60.6	387.9	224.3	140	28	wet	4.00	C
2012.7	3/29-4/10	82.1	512.5	297.3	80	51	wet	0.57	C
2012.8	4/15-5/13	81.6	196.5	139.0	7.5	1.7	dry	3.41	C

Event- water year and storm number of that water year, M^3/sec-cubic meters per second, Q_{min}-discharge at the start of storm event, Q_{max}-peak discharge of storm event, Q_{mid}-discharge at the midpoint of storm event, TU$_{RL}$-turbidity at the midpoint on the rising limb of the hydrograph, TU$_{FL}$- turbidity at the midpoint on the falling limb of the hydrograph,

HI-hysteresis index, HD-hysteresis direction, C-clockwise hysteresis (turbidity higher on rising limb of storm hydrograph),

CC-counter clockwise hysteresis (turbidity higher on the falling limb of the storm hydrograph)

Appendix F- Hysteresis Indices for Oregon City

Hysteresis Indices and Associated Data from Clackamas at Oregon City									
Event ID	WY 2006 Dates	Qmin (M³/sec)	Qmax (M³/sec)	Qmid (M³/sec)	Qrising (TURL)	Qfalling (TUFL)	Season	HI	HD
2006.1	11/10-11/24	73.1	186.9	130.0	4.8	1.4	wet	2.43	C
2006.2	12/18-12/26	34.8	186.3	110.6	23	23	wet	0.00	
2006.3	12/29-1/6	362.5	1305.4	833.9	120	100	wet	0.20	C
2006.6	1/27-2/11	74.8	218.3	146.5	30	52	wet	-0.73	CC
2006.7	2/27-3/5	65.1	142.2	103.6	21	3.7	wet	4.68	C
2006.8	3/7-3/12	83.8	113.8	98.8	24	4.2	wet	4.71	C
2006.9	4/2-4/30	81.0	211.8	146.4	7.8	4.1	Dry	0.90	C
Event ID	WY 2007 Dates	Qmin (M³/sec)	Qmax (M³/sec)	Qmid (M3/sec)	Qrising (TU$_{RL}$)	Qfalling (TU$_{FL}$)	Season	HI	HD
2007.2	12/8-12/22	84.4	557.8	321.1	20	30	Wet	-0.50	CC
2007.3	12/22-1/7	138.5	219.5	179.0	12	7.4	Wet	0.62	C
2007.6	3/24-4/1	109.0	286.0	197.5	29	4.9	Wet	4.92	C
Event ID	WY 2008 Dates	Qmin (M³/sec)	Qmax (M³/sec)	Qmid (M3/sec)	Qrising (TU$_{RL}$)	Qfalling (TU$_{FL}$)	Season	HI	HD
2008.1	10/15-10/26	28.9	162.3	95.6	9.7	2.7	Wet	2.59	C
2008.2	11/15-11/26	53.0	288.8	170.9	24	7	Wet	2.43	C

2008.3	12/1-12/16	69.9	841.0	455.5	45	40	Wet	0.13	C
2008.5	5/14-5/28	130.5	436.1	283.3	3.3	4.7	Dry	-0.42	CC

Event ID	WY 2009 Dates	Qmin (M^3/sec)	Qmax (M^3/sec)	Qmid (M3/sec)	Qrising (TU$_{RI}$)	Qfalling (TU$_{FL}$)	Season	HD	HI
2009.1	10/27-11/5	26.4	80.1	2.3	7	2.3	Wet	2.04	C
2009.2	11/5-11/18	48.4	688.1	368.3	50	31	Wet	0.61	C
2009.3	12/23-1/20	35.1	464.4	249.8	16	9.4	Wet	0.70	C
2009.4	2/21-3/17	45.6	252.3	148.9	4.2	8.1	Wet	-0.93	CC
2009.5	5/4-5/31	145.8	436.1	291.0	4.6	14	Dry	-2.04	CC

Event ID	WY 2010 Dates	Qmin (M^3/sec)	Qmax (M^3/sec)	Qmid (M3/sec)	Qrising (TU$_{RI}$)	Qfalling (TU$_{FL}$)	Season	HI	HD
2010.1	11/5 - 11/16	36.8	152.6	94.7	5.3	3.8	Wet	0.39	C
2010.2	12/9 - 12/30	36.5	245.2	140.9	15	4.5	Wet	2.33	C
2010.3	1/4 - 1/15	138.8	365.3	252.0	5.9	8.2	Wet	-0.39	CC
2010.4	3/28-4/5	89.8	549.3	319.6	34	23	Wet/Dry	0.48	C
2010.5	6/1 - 6/22	109.3	438.9	274.1	17	9.4	Dry	0.81	C
2010.6	9/14-10/2	20.2	54.7	37.4	0.9	1.3	Wet	-0.44	CC

Event ID	WY 2011 Dates	Qmin (M^3/sec)	Qmax (M^3/sec)	Qmid (M3/sec)	Qrising (TU$_{RI}$)	Qfalling (TU$_{FL}$)	Season	HI	HD
2011.2	11/13-11/26	72.8	280.9	176.8	30	8.4	Wet	2.57	C
2011.3	11/26-12/7	69.9	294.5	182.2	11	4.9	Wet	1.24	C
2011.4	12/7-12/25	85.8	753.2	419.5	43	31	Wet	0.39	C
2011.5	12/25-1/7	85.2	390.8	238.0	35	12	Wet	1.92	C
2011.6	1/11-2/2	68.8	1557.4	813.1	59	120	Wet	-1.03	CC

Event ID	WY 2012 Dates	Q_{min} (M^3/sec)	Q_{max} (M^3/sec)	Q_{mid} (M3/sec)	Qrising (TU$_{RL}$)	Qfalling (TU$_{FL}$)	Season	HI	HD
2011.7	4/14-4/24	132.8	351.1	242.0	4.6	7.9	Dry	-0.72	CC
2012.2	11/21-12/26	53.2	228.8	141.0	13	7.1	Wet	0.83	C
2012.3	12/27-1/16	35.4	906.1	470.8	110	82	Wet	0.34	C
2012.4	1/17-2/10	69.7	1226.1	647.9	65	36	Wet	0.81	C
2012.5	2/17-3/3	105.3	373.8	239.6	5.3	8.9	Wet	-0.68	CC
2012.6	3/9-3/27	132.0	727.7	429.8	21	25	Wet	-0.19	CC
2012.7	3/29-4/10	152.6	909.0	530.8	30	35	Wet/Dry	-0.17	CC
2012.8	4/15-5/13	132.8	305.8	219.3	5.9	5.8	Dry	0.02	C

Event- water year and storm number of that water year, WY-water year, M^3/sec-cubic meters per second, Q_{min}-discharge at the start of storm event, Q_{max}-peak discharge of storm event, Q_{mid}-discharge at the midpoint of storm event, TU$_{RL}$-turbidity at the midpoint on the rising limb of the hydrograph, TU$_{FL}$-turbidity at the midpoint on the falling limb of the hydrograph, HI-hysteresis index, HD-hysteresis direction, C-clockwise hysteresis (turbidity higher on rising limb of storm hydrograph), CC-counter clockwise hysteresis (turbidity higher on the falling limb of the storm hydrograph)

Appendix G-Shapiro-Wilk Test for Normality Results for Change in Turbidity Final Model Variables and Residuals

Shapiro-Wilk Test Results for Carter Bridge		
Site/Parameter	Shapiro-Wilk (SW)	SW p-value
Carter Bridge (LogΔQ)	0.9545	0.1087
Carter Bridge (LogΔTb)	0.9242	0.01048
Linear Model Residuals	0.9081	0.03322

Shapiro-Wilk Test Results for Oregon City		
Site/Parameter	Shapiro-Wilk (SW)	SW p-value
Oregon City (LogΔQ)	0.9817	0.7382
Oregon City (LogΔTb)	0.9552	0.1063
Linear Model Residuals	0.9308	0.0154